STABILIZED FINITE ELEMENT APPROXIMATIONS FOR A GENERALIZED BOUSSINESQ PROBLEM: A POSTERIORI ERROR ANALYSIS.

ALEJANDRO ALLENDES, CÉSAR NARANJO, AND ENRIQUE OTÁROLA

Abstract. The purpose of this work is the design and analysis of a posteriori error estimators for low-order stabilized finite element approximations of a generalized Boussinesq problem. We consider standard stabilization procedures over conforming finite element spaces and a nonconforming one that delivers a divergence-free discrete velocity field. The analysis, that is valid for two and three-dimensional domains, relies on a smallness assumption on the solution and is based on a technique that involves the Ritz projection of the residuals. The devised a posteriori error estimators are proven to be globally reliable and locally efficient. Three dimensional numerical experiments reveal a competitive performance of adaptive procedures driven by the designed a posteriori error estimators.

1. Introduction

In this work we will be interested in the design and analysis of a posteriori error estimators for a steady–state generalized Boussinesq problem [39, 42] which is a particular instance of an incompressible nonisothermal fluid flow model: it corresponds to a nonlinear system of partial differential equations (PDEs) that couples the stationary incompressible Navier–Stokes equations for the fluid variables (velocity and pressure) with a convection–diffusion equation for the temperature variable; the fluid viscosity and the thermal conductivity depend on the temperature of the fluid. To make matters precise, let Ω be an open and bounded domain of $\mathbb{R}^d$ ($d \in \{2,3\}$) with Lipchitz boundary $\partial\Omega$ and $\boldsymbol{g}$, $\boldsymbol{f}$, and h be given data. We shall be concerned with the following problem: Find $(\boldsymbol{u}, p, t)$ such that

$$\left\{\begin{array}{rcll} -\mathbf{div}(\varepsilon(t)\nabla\boldsymbol{u}) + \boldsymbol{u}\cdot\nabla\boldsymbol{u} + \nabla p - \boldsymbol{g}t &=& \boldsymbol{f} & \text{in } \Omega, \\ \operatorname{div}\boldsymbol{u} &=& 0 & \text{in } \Omega, \\ -\operatorname{div}(\kappa(t)\nabla t) + \boldsymbol{u}\cdot\nabla t &=& h & \text{in } \Omega, \\ \boldsymbol{u} &=& \boldsymbol{0} & \text{on } \Gamma, \\ t &=& 0 & \text{on } \Gamma, \end{array}\right. \tag{1}$$

where $\boldsymbol{u}$ denotes the fluid velocity, p the pressure, and t the temperature. The data of the problem is such that $\boldsymbol{f}, \boldsymbol{g} \in \boldsymbol{L}^2(\Omega)$ and $h \in L^2(\Omega)$. The functions ε and κ denote the fluid viscosity and the thermal conductivity, respectively; additional regularity requirements on ε and κ will be imposed in Section 3. A rather incomplete list of problems where the model (1) appears includes fume cupboard ventilation, heat exchangers, coolingof electronic equipments, cooling of nuclear reactors, climate predictions, oceanic flows, and many others.

To the best of our knowledge, the first work that propose and study solution techniques for the classical Boussinesq problem, which correspond to the special case of (1) where ε and ν are positive constants, is [13]. In this work, the authors obtain existence and, under a smallness assumption on the data, local uniqueness results. In addition, the authors propose a family of finite element solution techniques based on stable Stokes elements for the fluid variables and Lagrange elements for the temperature variable: the well–posedness of such discrete systems is obtained and rates of convergence are derived. Later, the authors of [24] propose a mixed formulation of the classical Boussinesq problem on two-dimensional polygonal domains: they study regularities properties of the solution and propose and analyze a mixed formulation where the gradients of the velocity and the temperature are introduced as new unknowns; quasi–optimal error estimates are provided. For further extensions and developments, we refer the reader to [4, 14, 16, 18, 19, 22, 28] and references therein.

A step in the analysis of the continuous problem (1), where the coefficients ε and κ are temperature-dependent, has been achieved in [30]. In this work, the authors study, under certain conditions on the temperature dependency of the viscosity and thermal conductivity, the existence and regularity of solutions of (1) using a spectral Galerkin method combined with fixed point arguments; see also [35]. On

Key words and phrases. a generalized Boussinesq problem; stabilized finite element methods; a posteriori error analysis, adaptive finite elements.

The first author was partially supported by CONICYT through FONDECYT project 1170579.

The third author was partially supported by CONICYT through FONDECYT project 11180193.

the basis of these results, the authors of [36] propose a conforming finite element method, prove its well–posedness [36, Proposition 3.1] and derive error estimates [36, Theorem 3.1] under a smallness assumption on the problem data. Later, an alternative approach is proposed in [33]: divergence-conforming Brezzi–Douglas–Marini (BDM) elements of order k for the approximation of the velocity, discontinuous elements of order $k-1$ for the pressure, and continuous elements of order k for the temperature. The resulting mixed finite element method has the distinct property that it yields exactly divergence-free velocity approximations. The authors derive optimal error estimates for problems with small and sufficiently smooth solutions [33, Section 5]. For further extensions and developments, we refer the reader to [5, 6, 7, 9, 34, 37] and references therein.

In an attempt to design and analyze an efficient solution technique for problem (1), specially on a three dimensional scenario, we will consider the so-called adaptive finite element methods (AFEMs). AFEMs are iterative methods that improve the quality of the finite element approximation to a PDE while striving to keep an optimal distribution of computational resources measured in terms of degrees of freedom. An essential ingredient of an AFEM is an a posteriori error estimator: a computable quantity that depends on the discrete solution and data, and provides information about the local quality of the approximate solution. Therefore, it can be used for adaptive mesh refinement and coarsening, error control and equidistribution of the computational effort. The a posteriori error analysis for standard finite element approximations of linear second-order elliptic boundary value problems has a solid foundation [41]. In contrast, the a posteriori error analysis of finite element discretizations of problem (1) has been much less explored. When ε and κ are constants and $d \in \{2,3\}$, the author of [4] propose and analyze, on the basis of the theory developed in [41], an a posteriori error estimator. He proved that the estimator is global reliable and locally efficient [4, Theorem 4.1]. We also mention the reference [43]. More recently, the authors of [20, 21], based on augmented fully-mixed formulations, present error estimators that are globally reliable and *globally* efficient; see [20, Theorems 3.1 and 3.13] and [21, Theorem 3.1]. When $d = 2$ and only the fluid viscocity ε is temperature dependent, an a posteriori error analysis has been recently performed in [8], where the authors prove that the devised error estimator is globally reliable [8, Theorem 3.1] and globally efficient [8, Theorem 3.13].

To the best of our knowledge, the a posteriori error analysis for problem (1), where $d \in \{2,3\}$ and both the fluid viscosity and the thermal conductivity depend on the temperature of the fluid, has not been considered before. This is the main contribution of our work. Since the numerical resolution of problem (1) is a dauting task, based on [5], we approximate the solution to (1) with low-order conforming stabilized finite element schemes. To derive the global reliability of the proposed a posteriori error estimators we invoke the ideas developed in [2] and prove that the total error is bounded by the energy norm of the Ritz projection of the residuals; see Theorem 29. In Theorems 4 and 5, and under particular elections of the stabilization terms, we prove that the designed error estimators are globally reliable. The *local* efficiency of our error estimators follow standard arguments [41]. We also include an a posteriori error analysis for a particular nonconforming scheme with a post-processed final solution which has the advantage of being solenoidal.

The outline of this paper is as follows. In Section 2 we introduce some terminology used throughout this work. In Section 3 we introduce the generalized Boussinesq problem that we will study: we review the main properties of the forms involved in the formulation and a result about existence of solutions. We also derive a uniqueness result under a smallness assumption on the continuous variables and data. In Section 4, we introduce stabilization procedures over conforming finite element spaces and a nonconforming one that delivers a divergence-free discrete velocity field. The core of our work is Section 5, where, in section 5.1, we provide an estimate for the total error in terms of the energy norm of the Ritz projection of the residuals which we utilize, in Section 5.2, to derive reliability estimates for the devised a posteriori error estimators. Efficiency estimates for such estimators are derived in Section 5.4. Finally, in section 6 we present a series of numerical examples in three dimensions that illustrate the theory.

2. Notation and preliminaries

Let us set notation and describe the setting we shall operate with. Throughout this work $d \in \{2,3\}$ and $\Omega \subset \mathbb{R}^d$ is an open and bounded polytopal domain with Lipschitz boundary $\Gamma := \partial\Omega$.

We shall use standard notation for Lebesgue and Sobolev spaces, norms, and inner products. For an open and bounded domain $\mathcal{O} \subset \mathbb{R}^d$ ($d = 2,3$), $r \geq 0$, and $p \in [1,\infty]$, $L^p(\mathcal{O})$ denotes the space of p-integrable functions over $\mathcal{O}$ and $W^{r,p}(\mathcal{O})$ the usual Sobolev space. We denote by $\|\cdot\|_{L^p(\mathcal{O})}$ and $\|\cdot\|_{W^{r,p}(\mathcal{O})}$ the classical norms on $L^p(\mathcal{O})$ and $W^{r,p}(\mathcal{O})$, respectively. When $r = 2$, $W^{r,p}(\mathcal{O})$ is the Hilbert space $H^r(\mathcal{O})$, for which we denote by $\|\cdot\|_{H^r(\mathcal{O})}$ its norm and by $|\cdot|_{H^r(\mathcal{O})}$ its seminorm. We use bold letters to denote the vector-valued counterparts of the aforementioned spaces and an extra underaccent

for their matrix-valued counterparts. We denote by $\boldsymbol{X}(\Omega)$ the space of functions that belong to $\boldsymbol{H}^1_0(\mathcal{O})$ and are solenoid; $\boldsymbol{H}(\mathbf{div},\mathcal{O})$ stands for the space of functions that belongs to $\boldsymbol{L}^2(\mathcal{O})$ whose divergence belongs to $L^2(\mathcal{O})$.

We now proceed to define notation associated with the discretization of the domain. Let $\mathscr{T} = \{K\}$ be a shape-regular partition of $\bar{\Omega}$ into simplicial elements K in the sense of Ciarlet [17].

For a fixed partition $\mathscr{T}$, let $\mathcal{F}$ denote the set of all element edges(2D)/faces(3D), $\mathcal{F}_I \subset \mathcal{F}$ denote the set of interior edges(2D)/faces(3D), and $\mathcal{V}$ index the set $\{\boldsymbol{x}_n\}$ of all the vertices in the mesh.

For an element $K \in \mathscr{T}$, let

- $\mathbb{P}_n(K)$ denotes the space of polynomials on K of total degree at most n;
- $\mathcal{F}_K \subset \mathcal{F}$ denotes the set containing the individual edges(2D)/faces(3D) of K;
- $|K|$ denotes the area(2D)/volume(3D) of K;
- h_K denote the diameter of K;
- $\boldsymbol{n}^K_\gamma$ denotes the unit exterior normal to the edge(2D)/face(3D) $\gamma \in \mathcal{F}_K$;
- $\boldsymbol{v}_{|K}$ denotes the restriction of $\boldsymbol{v}$ to the element K.

For an edge(2D)/face(3D) $\gamma \in \mathcal{F}$, let

- $|\gamma|$ denotes the length(2D)/area(3D) of the edge(2D)/face(3D) γ;
- h_γ denotes the diameter of the edge(2D)/face(3D) γ;
- $\Omega_\gamma = \{K \in \mathscr{T} : \gamma \in \mathcal{F}_K\}$;
- $\boldsymbol{v}_{|\gamma}$ denotes the restriction of $\boldsymbol{v}$ to the edge(2D)/face(3D) γ;
- $\boldsymbol{\varphi}_\gamma$ denotes the lowest order Raviart-Thomas basis function satisfying, for all $\gamma \in \mathcal{F}_I \cap \mathcal{F}_K$, that

$$\boldsymbol{\varphi}_\gamma(\boldsymbol{x}) = \pm\frac{|\gamma|}{d|K|}(\boldsymbol{x}-\boldsymbol{x}_\gamma), \quad \mathbf{div}\,\boldsymbol{\varphi}_\gamma = \pm\frac{|\gamma|}{|K|}, \quad \nabla\boldsymbol{\varphi}_{\gamma|K} = \pm\frac{|\gamma|}{d|K|}\mathbf{I}, \quad \|\nabla\boldsymbol{\varphi}_\gamma\|^2_{\boldsymbol{L}^2(K)} \leq Ch_\gamma^{d-2}, \tag{2}$$

  where $\boldsymbol{x}_\gamma$ correspond to the vertex opposite to the edge(2D)/face(3D) γ and $\mathbf{I}$ is the identity matrix. The signs $\pm$ are chosen by fixing a normal vector for every $\gamma \in \mathcal{F}_I$, as depicted in Figure 1, and $C > 0$ is independent of any mesh size; we also notice that $\boldsymbol{\varphi}_{\gamma|\gamma'} \cdot \boldsymbol{n}_{\gamma'} = 0$ for all $\gamma, \gamma' \in \mathcal{F}_K$ with $\gamma \neq \gamma'$.
- $[\![\phi]\!]_\gamma$, on $\gamma = \mathcal{F}_{K^+} \cap \mathcal{F}_{K^-}$, denotes the jump of the function ϕ, which is defined by fixing a normal vector for every $\gamma \in \mathcal{F}_I$, based on Figure 1, as

$$[\![\phi]\!]_\gamma = \phi_{K^+} - \phi_{K^-}. \tag{3}$$

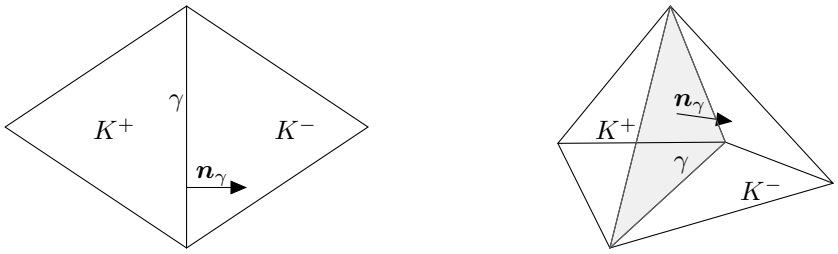

FIGURE 1. For $\gamma = \mathcal{F}_{K^+} \cap \mathcal{F}_{K^-}$, by fixing a normal vector $\boldsymbol{n}_\gamma$ pointing from K^+ to K^-, the lowest order Raviart–Thomas basis function and inter element jumps are defined.

For $n \in \mathcal{V}$, we let λ_n denote the continuous, piecewise linear basis function associated to the vertex $\boldsymbol{x}_n$, characterized by the conditions $\lambda_n \in \mathbb{P}_1(K)$ for all $K \in \mathscr{T}$ and $\lambda_n(\boldsymbol{x}_m) = \delta_{nm}$ for all $m \in \mathcal{V}$, where δ_{nm} denotes the Kronecker symbol.

We introduce the broken Sobolev space

$$H^1(\mathscr{T}) := \left\{\phi : \phi_{|K} \in H^1(K) \;\forall\; K \in \mathscr{T}\right\}$$

and the finite element spaces

$$V(\mathscr{T}) := \{v \in \mathcal{C}(\overline{\Omega}) :\; v_{|K} \in \mathbb{P}_1(K) \;\forall\; K \in \mathscr{T}\} \cap H^1_0(\Omega),$$
$$Q(\mathscr{T}) := \{q \in L^2_0(\Omega) :\; q_{|K} \in \mathbb{P}_0(K) \;\forall\; K \in \mathscr{T}\}.$$

For $K \in \mathscr{T}$ and nonnegative integers ℓ, we denote by $\Pi_{K,\ell}$ the $L^2(K)$-orthogonal projection operator onto $\mathbb{P}_\ell(K)$. This operator is defined as

$$(v - \Pi_{K,\ell}(v), w)_{L^2(K)} = 0 \quad \forall\; w \in \mathbb{P}_\ell(K).$$

The vector countepart will be denoted by $\boldsymbol{\Pi}_{K,\ell}$.

Throughout the manuscript we will frequently make use of the following inequalities. First, a Poincaré inequality, that is valid for $v \in H^1_0(\Omega)$, and second, a standard Sobolev embedding estimate, that holds for $w \in H^1(\Omega)$ and $p \in [1,\infty)$ for $d = 2$ and $p \in [1,6]$ for $d = 3$:

$$\|v\|_{L^2(\Omega)} \leq C_{P,\Omega}|v|_{H^1(\Omega)}, \qquad \|w\|_{L^p(\Omega)} \leq C_{p,\Omega}\|w\|_{H^1(\Omega)}; \tag{4}$$

their obvious extensions being considered for vector-valued functions. In the latter case and for simplicity, we maintain the same notation for the involved constants with the convention that for the analysis that follows we will choose the one with maximum value.

Finally, in the manuscript we shall use C to denote a positive constant that is independent of the size of the elements in the mesh and whose value may change whenever it is written in two different places.

3. Model problem

We consider the following generalized Boussinesq problem: Find $(\boldsymbol{u}, p, t)$ such that

$$\left\{\begin{array}{rcll} -\mathbf{div}(\varepsilon(t)\nabla\boldsymbol{u}) + \boldsymbol{u}\cdot\nabla\boldsymbol{u} + \nabla p - \boldsymbol{g}t &=& \boldsymbol{f} & \text{in } \Omega, \\ \operatorname{div}\boldsymbol{u} &=& 0 & \text{in } \Omega, \\ -\operatorname{div}(\kappa(t)\nabla t) + \boldsymbol{u}\cdot\nabla t &=& h & \text{in } \Omega, \\ \boldsymbol{u} &=& \boldsymbol{0} & \text{on } \Gamma, \\ t &=& 0 & \text{on } \Gamma, \end{array}\right. \tag{5}$$

where $\boldsymbol{u}$ denotes the fluid velocity, p the pressure, and t the temperature. The data of the problem is such that $\boldsymbol{f}, \boldsymbol{g} \in \boldsymbol{L}^2(\Omega)$ and $h \in L^2(\Omega)$. The functions ε and κ denote the fluid viscosity and the thermal conductivity, respectively. We assume that ε and κ strictly positive and uniformly bounded:

$$0 < \varepsilon_1 \leq \varepsilon(t) \leq \varepsilon_2, \quad 0 < \kappa_1 \leq \kappa(t) \leq \kappa_2, \quad \text{a.e. in } \Omega, \quad \forall\, t \in H^1(\Omega). \tag{6}$$

In addition, we assume that ε and κ are Lipschitz: there exist constants $\varepsilon_{lip} > 0$ and $\kappa_{lip} > 0$ such that

$$|\varepsilon(t_1) - \varepsilon(t_2)| \leq \varepsilon_{lip}|t_1 - t_2|, \quad |\kappa(t_1) - \kappa(t_2)| \leq \kappa_{lip}|t_1 - t_2|, \quad \text{a.e. in } \Omega, \quad \forall\, t_1, t_2 \in H^1(\Omega). \tag{7}$$

Remark (nonhomogeneous Dirichlet boundary conditions). To simplify the presentation of the material, in this work we will only consider homogeneous Dirichlet boundary conditions. The case of nonhomogenous Dirichlet boundary conditions for the continuous problem, as it is customary, can be treated by a change of variable which leads to modifications in the right-hand sides of (5); see [13, 30]. We also mention that, from the discrete point of view, in [34] the authors consider a nonhomogeneous Dirichlet boundary condition for the temperature variable which is weakly imposed in the overall weak system; the latter being optimally approximated by standard conforming finite element spaces.

The weak formulation of (5) reads as follows: Find $(\boldsymbol{u}, p, t) \in \boldsymbol{H}^1_0(\Omega) \times L^2_0(\Omega) \times H^1_0(\Omega)$ such that

$$\left\{\begin{array}{rcll} \mathcal{A}(t;\boldsymbol{u},\boldsymbol{v}) + \mathcal{C}(\boldsymbol{u};\boldsymbol{u},\boldsymbol{v}) - \mathcal{B}(\boldsymbol{v},p) - \mathcal{D}(t,\boldsymbol{v}) &=& \mathcal{F}(\boldsymbol{v}) & \forall\, \boldsymbol{v} \in \boldsymbol{H}^1_0(\Omega), \\ \mathcal{B}(\boldsymbol{u},q) &=& 0 & \forall\, q \in L^2_0(\Omega), \\ \mathscr{A}(t;t,w) + \mathscr{C}(\boldsymbol{u};t,w) &=& \mathcal{H}(w) & \forall\, \boldsymbol{w} \in H^1_0(\Omega). \end{array}\right. \tag{8}$$

The involved forms in (8) are defined as

$$\begin{aligned} \mathcal{A}(r;\boldsymbol{v},\boldsymbol{w}) &:= \int_\Omega \varepsilon(r)\nabla\boldsymbol{v} : \nabla\boldsymbol{w}, \quad \mathcal{C}(\boldsymbol{r};\boldsymbol{v},\boldsymbol{w}) := \int_\Omega (\boldsymbol{r}\cdot\nabla\boldsymbol{v})\cdot\boldsymbol{w}, \quad \mathcal{B}(\boldsymbol{v},q) := \int_\Omega q\,\mathbf{div}\,\boldsymbol{v}, \\ \mathcal{D}(r,\boldsymbol{v}) &:= \int_\Omega r\,\boldsymbol{g}\cdot\boldsymbol{v}, \quad \mathscr{A}(r;v,w) := \int_\Omega \kappa(r)\nabla v\cdot\nabla w, \quad \mathscr{C}(\boldsymbol{r};v,w) := \int_\Omega (\boldsymbol{r}\cdot\nabla v)w. \end{aligned} \tag{9}$$

In addition,

$$\mathcal{F}(\boldsymbol{v}) := \int_\Omega \boldsymbol{f}\cdot\boldsymbol{v}, \quad \mathcal{H}(w) := \int_\Omega hw. \tag{10}$$

The existence of solutions for problem (8) follows from [30, Theorem 2.1]: If $\partial\Omega$ is Lipschitz, the functions ε and κ are continuous, $\boldsymbol{f}, \boldsymbol{g} \in \boldsymbol{L}^2(\Omega)$, and $h \in L^2(\Omega)$, then there exists a weak solution for problem (8). Stricly speaking [30, Theorem 2.1] only shows the existence of a weak solution for (8) when $\boldsymbol{f} = 0$ and $h = 0$. However, from a slight modification of the argumentes presented in [30], we can conclude the existence of weak solutions when $\boldsymbol{f} \neq \boldsymbol{0}$ and $h \neq 0$.

3.1. **Stability properties.** This section is devoted to list a series of continuity, coercivity, and inf–sup properties of the forms defined in (9). First, in view of (6), we immediately conclude the coercivity of the bilinear forms $\mathcal{A}$ and $\mathscr{A}$. In fact,

$$\varepsilon_1|\boldsymbol{v}|^2_{\boldsymbol{H}^1(\Omega)} \leq \mathcal{A}(r;\boldsymbol{v},\boldsymbol{v}), \qquad \kappa_1|v|^2_{H^1(\Omega)} \leq \mathscr{A}(r;v,v) \tag{11}$$

for all $\boldsymbol{v} \in \boldsymbol{H}^1_0(\Omega)$, $v \in H^1_0(\Omega)$ and $r \in H^1(\Omega)$. Second, invoking (6), again, which guarantees that ε and κ are bounded, we conclude that

$$|\mathcal{A}(r;\boldsymbol{v},\boldsymbol{w})| \leq \varepsilon_2|\boldsymbol{v}|_{\boldsymbol{H}^1(\Omega)}|\boldsymbol{w}|_{\boldsymbol{H}^1(\Omega)}, \quad |\mathscr{A}(r;v,w)| \leq \kappa_2|v|_{H^1(\Omega)}|w|_{H^1(\Omega)} \tag{12}$$

for all $\boldsymbol{v},\boldsymbol{w} \in \boldsymbol{H}^1_0(\Omega)$, $v,w \in H^1_0(\Omega)$, and $r \in H^1(\Omega)$. Third, an application of the Sobolev embedding $L^4(\Omega) \hookrightarrow H^1(\Omega)$ combined with the Hölder's inequality yield

$$\mathcal{C}(\boldsymbol{r};\boldsymbol{v},\boldsymbol{w}) \leq C_{D,\Omega}|\boldsymbol{r}|_{\boldsymbol{H}^1(\Omega)}|\boldsymbol{v}|_{\boldsymbol{H}^1(\Omega)}|\boldsymbol{w}|_{\boldsymbol{H}^1(\Omega)}, \quad \mathscr{C}(\boldsymbol{r};v,w) \leq C_{D,\Omega}|\boldsymbol{r}|_{\boldsymbol{H}^1(\Omega)}|v|_{H^1(\Omega)}|w|_{H^1(\Omega)}, \tag{13}$$

for all $\boldsymbol{r},\boldsymbol{v},\boldsymbol{w} \in \boldsymbol{H}^1_0(\Omega)$ and $v,w \in H^1_0(\Omega)$. The constant $C_{D,\Omega}$ is defined as

$$C_{D,\Omega} := C^2_{4,\Omega}(1 + C^2_{P,\Omega}). \tag{14}$$

Fourth, invoking the Lipschitz property that ε and κ satisfy and utilizing Hölder's inequality combined with the Sobolev embedding $L^6(\Omega) \hookrightarrow H^1(\Omega)$ we arrive at

$$\begin{aligned} |\mathcal{A}(t_1;\boldsymbol{v},\boldsymbol{w}) - \mathcal{A}(t_2;\boldsymbol{v},\boldsymbol{w})| &\leq \varepsilon_{lip}\mathfrak{C}_\Omega|t_1 - t_2|_{H^1(\Omega)}\|\nabla\boldsymbol{v}\|_{\boldsymbol{L}^3(\Omega)}|\boldsymbol{w}|_{\boldsymbol{H}^1(\Omega)}, \\ |\mathscr{A}(t_1;v,w) - \mathscr{A}(t_2;v,w)| &\leq \kappa_{lip}\mathfrak{C}_\Omega|t_1 - t_2|_{H^1(\Omega)}\|\nabla v\|_{L^3(\Omega)}|w|_{H^1(\Omega)}, \end{aligned} \tag{15}$$

for all $\boldsymbol{v} \in \boldsymbol{W}^{1,3}_0(\Omega)$, $\boldsymbol{w} \in \boldsymbol{H}^1_0(\Omega)$, $v \in W^{1,3}_0(\Omega)$, $w \in H^1_0(\Omega)$, and $t_1,t_2 \in H^1(\Omega)$. Here, $\mathfrak{C}_\Omega = C_{6,\Omega}(1 + C^2_{P,\Omega})^{\frac{1}{2}}$. Fifth, for $\boldsymbol{s} \in \boldsymbol{X}(\Omega)$, $\boldsymbol{v} \in \boldsymbol{H}^1_0(\Omega)$ and $v \in H^1_0(\Omega)$, we have that

$$\mathcal{C}(\boldsymbol{s};\boldsymbol{v},\boldsymbol{v}) = 0, \qquad \mathscr{C}(\boldsymbol{s};v,v) = 0. \tag{16}$$

Sixth, for $\boldsymbol{g},\boldsymbol{v} \in \boldsymbol{H}^1(\Omega)$ and $r \in H^1(\Omega)$, we have that

$$\mathcal{D}(r,\boldsymbol{v}) \leq C_{D,\Omega}\|\boldsymbol{g}\|_{\boldsymbol{L}^2(\Omega)}|r|_{H^1(\Omega)}|\boldsymbol{v}|_{\boldsymbol{H}^1(\Omega)}. \tag{17}$$

Finally, the bilinear form $\mathcal{B}$ satisfies the inf–sup condition [23, 26]

$$\sup_{\boldsymbol{v}\in\boldsymbol{H}^1_0(\Omega)\setminus\{\boldsymbol{0}\}} \frac{\mathcal{B}(\boldsymbol{v},q)}{|\boldsymbol{v}|_{\boldsymbol{H}^1(\Omega)}} \geq \beta\|q\|_{L^2(\Omega)} \quad \forall\, q \in L^2_0(\Omega). \tag{18}$$

3.2. **A uniqueness result.** In what follows we derive an uniqueness result for problem (8). To accomplish this task, we rewrite (8) as the following restricted problem [26]: Find $(\boldsymbol{u},t) \in \boldsymbol{X}(\Omega) \times H^1_0(\Omega)$ such that

$$\left\{ \begin{array}{rcll} \mathcal{A}(t;\boldsymbol{u},\boldsymbol{v}) + \mathcal{C}(\boldsymbol{u};\boldsymbol{u},\boldsymbol{v}) - \mathcal{D}(t,\boldsymbol{v}) &=& \mathcal{F}(\boldsymbol{v}) & \forall\, \boldsymbol{v} \in \boldsymbol{X}(\Omega), \\ \mathscr{A}(t;t,w) + \mathscr{C}(\boldsymbol{u};t,w) &=& \mathcal{H}(w) & \forall\, w \in H^1_0(\Omega). \end{array} \right. \tag{19}$$

A unique pressure $p \in L^2_0(\Omega)$ can be obtained in view of de Rham's Theorem [23, Theorem B.73].

We now present a uniqueness result that follows standard arguments. When compared with [33, Theorem 2.3], our result improves upon regularity: it demands $(\boldsymbol{u},t) \in \boldsymbol{W}^{1,3}(\Omega) \times W^{1,3}(\Omega)$. Similarly, it requires a smallness assumption on the continuous variables; the latter being crucial in order to perform an a posteriori error analysis; see Theorem 2.

Theorem 1 (uniqueness)**.** *Let $(\boldsymbol{u},t) \in [\boldsymbol{X}(\Omega) \cap \boldsymbol{W}^{1,3}(\Omega)] \times [H^1_0(\Omega) \cap W^{1,3}(\Omega)]$ be a solution to* (19)*, and assume that*

$$\max\left\{\|\boldsymbol{g}\|_{\boldsymbol{L}^2(\Omega)}, |\boldsymbol{u}|_{\boldsymbol{W}^{1,\ell}(\Omega)}, |t|_{W^{1,\ell}(\Omega)}\right\} < M := \min\left\{\frac{\varepsilon_1}{2C_{D,\Omega}}, \frac{\kappa_1}{(\kappa_{lip}+\varepsilon_{lip})\mathfrak{C}_\Omega + C_{D,\Omega}}\right\}, \tag{20}$$

where $\ell \in \{2,3\}$. Then, problem (8) *admits a unique solution.*

Proof. Let us assume that there exist two solutions $(\boldsymbol{u},t)$ and $(\boldsymbol{u}^*,t^*)$ of (19) that satisfy (20). Subtracting the corresponding variational formulations we arrive at

$$[\mathcal{A}(t;\boldsymbol{u},\boldsymbol{v}) - \mathcal{A}(t^*;\boldsymbol{u}^*,\boldsymbol{v})] + [\mathcal{C}(\boldsymbol{u};\boldsymbol{u},\boldsymbol{v}) - \mathcal{C}(\boldsymbol{u}^*;\boldsymbol{u}^*,\boldsymbol{v})] - \mathcal{D}(t-t^*,\boldsymbol{v}) = 0 \quad \forall\, \boldsymbol{v} \in \boldsymbol{X}(\Omega), \tag{21}$$

and that

$$[\mathscr{A}(t;t;w) - \mathscr{A}(t^*;t^*,w)] + [\mathscr{C}(\boldsymbol{u};t,w) - \mathscr{C}(\boldsymbol{u}^*;t^*,w)] = 0 \quad \forall\, w \in H^1_0(\Omega). \tag{22}$$

Since $\mathcal{A}$, $\mathcal{C}$, $\mathscr{A}$, and $\mathscr{C}$ are linear in the second and third argument, we can thus write the following expressions:

$$\begin{aligned}
\mathcal{A}(t;\boldsymbol{u},\boldsymbol{v}) - \mathcal{A}(t^*;\boldsymbol{u}^*,\boldsymbol{v}) &= \mathcal{A}(t;\boldsymbol{u}-\boldsymbol{u}^*,\boldsymbol{v}) + \left[\mathcal{A}(t;\boldsymbol{u}^*,\boldsymbol{v}) - \mathcal{A}(t^*;\boldsymbol{u}^*,\boldsymbol{v})\right],\\
\mathcal{C}(\boldsymbol{u};\boldsymbol{u},\boldsymbol{v}) - \mathcal{C}(\boldsymbol{u}^*;\boldsymbol{u}^*,\boldsymbol{v}) &= \mathcal{C}(\boldsymbol{u};\boldsymbol{u}-\boldsymbol{u}^*,\boldsymbol{v}) + \mathcal{C}(\boldsymbol{u}-\boldsymbol{u}^*;\boldsymbol{u}^*,\boldsymbol{v}),\\
\mathscr{A}(t;t;w) - \mathscr{A}(t^*;t^*,w) &= \mathscr{A}(t;t-t^*;w) + \left[\mathscr{A}(t;t^*,w) - \mathscr{A}(t^*;t^*,w)\right],\\
\mathscr{C}(\boldsymbol{u};t,w) - \mathscr{C}(\boldsymbol{u}^*;t^*,w) &= \mathscr{C}(\boldsymbol{u};t-t^*,w) + \mathscr{C}(\boldsymbol{u}-\boldsymbol{u}^*;t^*,w).
\end{aligned}$$

Set $\boldsymbol{v} = \boldsymbol{u} - \boldsymbol{u}^* \in \boldsymbol{X}(\Omega)$ in (21) and invoke (11) and (16) to conclude that

$$\begin{aligned}
\varepsilon_1 |\boldsymbol{u}-\boldsymbol{u}^*|^2_{\boldsymbol{H}^1(\Omega)} &\leq |\mathcal{A}(t;\boldsymbol{u}^*,\boldsymbol{u}-\boldsymbol{u}^*) - \mathcal{A}(t^*;\boldsymbol{u}^*,\boldsymbol{u}-\boldsymbol{u}^*)| + |\mathcal{C}(\boldsymbol{u}-\boldsymbol{u}^*;\boldsymbol{u}^*,\boldsymbol{u}-\boldsymbol{u}^*)| + |\mathcal{D}(t-t^*,\boldsymbol{u}-\boldsymbol{u}^*)|\\
&\leq \varepsilon_{lip}\mathfrak{C}_\Omega M |t-t^*|_{H^1(\Omega)} |\boldsymbol{u}-\boldsymbol{u}^*|_{\boldsymbol{H}^1(\Omega)} + C_{D,\Omega} M |\boldsymbol{u}-\boldsymbol{u}^*|^2_{\boldsymbol{H}^1(\Omega)} + C_{D,\Omega} M |t-t^*|_{H^1(\Omega)} |\boldsymbol{u}-\boldsymbol{u}^*|_{\boldsymbol{H}^1(\Omega)},
\end{aligned}$$

where we have also used (15), (13), (17), and the smallness assumption (20). This immediately implies that

$$\left(\varepsilon_1 - C_{D,\Omega} M\right) |\boldsymbol{u}-\boldsymbol{u}^*|_{\boldsymbol{H}^1(\Omega)} - \left(\varepsilon_{lip}\mathfrak{C}_\Omega M + C_{D,\Omega} M\right) |t-t^*|_{H^1(\Omega)} \leq 0. \tag{23}$$

Similarly, set $w = t - t^*$ in (22). Notice that, since $\boldsymbol{u} \in \boldsymbol{X}(\Omega)$, $\mathscr{C}(\boldsymbol{u};t-t^*,t-t^*) = 0$. Then,

$$\begin{aligned}
\kappa_1 |t-t^*|^2_{H^1(\Omega)} &\leq |\mathscr{A}(t;t^*,t-t^*) - \mathscr{A}(t^*;t^*,t-t^*)| + |\mathscr{C}(\boldsymbol{u}-\boldsymbol{u}^*;t^*,t-t^*)|\\
&\leq \kappa_{lip}\mathfrak{C}_\Omega M |t-t^*|^2_{H^1(\Omega)} + C_{D,\Omega} M |\boldsymbol{u}-\boldsymbol{u}^*|_{\boldsymbol{H}^1(\Omega)} |t-t^*|_{H^1},
\end{aligned}$$

which immediately yields

$$- C_{D,\Omega} M |\boldsymbol{u}-\boldsymbol{u}^*|_{\boldsymbol{H}^1(\Omega)} + \left(\kappa_1 - \kappa_{lip}\mathfrak{C}_\Omega M\right) |t-t^*|_{H^1(\Omega)} \leq 0. \tag{24}$$

Adding (23) and (24), we conclude that

$$\left(\varepsilon_1 - 2C_{D,\Omega} M\right) |\boldsymbol{u}-\boldsymbol{u}^*|_{\boldsymbol{H}^1(\Omega)} + \left(\kappa_1 - ((\kappa_{lip}+\varepsilon_{lip})\mathfrak{C}_\Omega + C_{D,\Omega})M\right) |t-t^*|_{H^1(\Omega)} \leq 0.$$

The result then follows from the use of assumption (20). This concludes the proof. □

Remark (regularity of $\mathbf{u}$ and t). In what follows we will assume that solutions to problem (5) are such that $(\boldsymbol{u},t) \in \boldsymbol{W}^{1,3}(\Omega) \times W^{1,3}(\Omega)$. We mention that, when the simplified case $\varepsilon \equiv 1$ and $\kappa \equiv 1$ takes place, a proof of such a regularity result can be obtained upon invoking the results of [32]. In fact, based on [27, Section 7.3.3] and [38, Chapter II, Section 1.3], let us consider the homogeneous problem for the incompressible Stokes system with Dirichlet boundary conditions:

$$\begin{cases}
-\Delta\boldsymbol{\varphi} + \nabla\psi = \boldsymbol{\tau}, & \text{in } \Omega,\\
\mathrm{div}\boldsymbol{\varphi} = 0, & \text{in } \Omega,\\
\boldsymbol{\varphi} = 0, & \text{on } \partial\Omega,
\end{cases}$$

and define the associated Green operator as $G_D\boldsymbol{\tau} = \boldsymbol{\varphi}$. The authors of [32] have proved that, if Ω is a bounded and Lipschitz domain, then the Green operator G_D is bounded from $\boldsymbol{W}^{-1,p}(\Omega)$ into $\boldsymbol{W}^{1,p}(\Omega)$ for $p \in (2n/(n+1) - \epsilon, 2n/(n-1) + \epsilon)$ and $\epsilon = \epsilon(\Omega) > 0$. With this result at hand, and invoking a similar argument based on the regularity results of [29, Theorem 0.5] (see also [29, 31]), the fact that $(\boldsymbol{u},t) \in \boldsymbol{W}^{1,3}(\Omega) \times W^{1,3}(\Omega)$ thus follows.

4. Stabilized finite element discretizations

To approximate the solution of problem (8) we will consider the following two stabilized finite element approximations.

4.1. A conforming low order method (SFEM1).

First, we introduce the following low-order stabilized finite element approximation: Find $(\boldsymbol{u}_{\mathscr{T}}, p_{\mathscr{T}}, t_{\mathscr{T}}) \in \boldsymbol{V}(\mathscr{T}) \times Q(\mathscr{T}) \times V(\mathscr{T})$ such that

$$\left\{\begin{aligned}
\mathcal{A}(t_{\mathscr{T}};\boldsymbol{u}_{\mathscr{T}},\boldsymbol{v}_{\mathscr{T}}) + \mathcal{C}(\boldsymbol{u}_{\mathscr{T}};\boldsymbol{u}_{\mathscr{T}},\boldsymbol{v}_{\mathscr{T}}) - \mathcal{B}(\boldsymbol{v}_{\mathscr{T}},p_{\mathscr{T}}) + \mathcal{S}_F(\boldsymbol{u}_{\mathscr{T}},\boldsymbol{v}_{\mathscr{T}}) - \mathcal{G}(t_{\mathscr{T}},\boldsymbol{v}_{\mathscr{T}}) &= \mathcal{F}(\boldsymbol{v}_{\mathscr{T}})\\
\mathcal{B}(\boldsymbol{u}_{\mathscr{T}},q_{\mathscr{T}}) + \sum_{\gamma\in\mathcal{F}_I} \frac{h_\gamma}{12}\int_\gamma [\![p_{\mathscr{T}}]\!]_\gamma [\![q_{\mathscr{T}}]\!]_\gamma &= 0\\
a(t_{\mathscr{T}};t_{\mathscr{T}},w_{\mathscr{T}}) + c(\boldsymbol{u}_{\mathscr{T}};t_{\mathscr{T}},w_{\mathscr{T}}) + \mathcal{S}_T(t_{\mathscr{T}},w_{\mathscr{T}}) &= \mathcal{H}(w_{\mathscr{T}}),
\end{aligned}\right. \tag{25}$$

for all $(\boldsymbol{v}_{\mathscr{T}}, q_{\mathscr{T}}, w_{\mathscr{T}}) \in \boldsymbol{V}(\mathscr{T}) \times Q(\mathscr{T}) \times V(\mathscr{T})$. In (25), $\mathcal{S}_F(\cdot,\cdot)$ and $\mathcal{S}_T(\cdot,\cdot)$ denote linear stabilization terms associated to the fluid and temperature equations, respectively. We will assume that $\mathcal{S}_F$ and $\mathcal{S}_T$ are such that a unique solution to problem (25) exists.

An a priori error analysis for a slight variation of the scheme (25) has been recently performed in [5]. We also mention [34], where the authors investigate an scheme for (5) based on stable Stokes elements

for the fluid variables and Lagrange elements for the temperature variable; no stabilization terms are considered.

4.2. **A nonconforming low order divergence-free solution (SFEM2).** The second solution technique is based on (25). In fact, when the solution to the discrete problem (25) is computed, we consider, as a final solution, the triple $(\mathfrak{L}(\boldsymbol{u}_{\mathscr{T}}, p_{\mathscr{T}}), p_{\mathscr{T}}, t_{\mathscr{T}})$, where $\mathfrak{L}(\boldsymbol{u}_{\mathscr{T}}, p_{\mathscr{T}})$ is defined as follows:

$$\mathfrak{L}(\boldsymbol{u}_{\mathscr{T}}, p_{\mathscr{T}}) := \boldsymbol{u}_{\mathscr{T}} + \sum_{\gamma \in \mathcal{F}_I} \frac{h_\gamma}{12} [\![p_{\mathscr{T}}]\!]_\gamma \boldsymbol{\varphi}_\gamma, \tag{26}$$

where φ_γ denotes the Raviart-Thomas basis function defined in (2); notice that the discrete variables $p_{\mathscr{T}}$ and $t_{\mathscr{T}}$ are not modified. The main advantage of this postprocessing step is that the final velocity approximation is solenoidal [5, Theorem 1]. This is,

$$\mathbf{div}\, \mathfrak{L}(\boldsymbol{u}_{\mathscr{T}}, p_{\mathscr{T}}) = 0 \quad \text{in } \Omega. \tag{27}$$

In practice this could be of interest since, as the numerical experiments of [5, Section 6] reveal, the triple $(\mathfrak{L}(\boldsymbol{u}_{\mathscr{T}}, p_{\mathscr{T}}), p_{\mathscr{T}}, t_{\mathscr{T}})$ seems to be a more accurate solution than $(\boldsymbol{u}_{\mathscr{T}}, p_{\mathscr{T}}, t_{\mathscr{T}})$.

5. A posteriori error analysis

In this section we analyze a posterior error estimates for the finite element scheme (25) that approximates the solution to (8). To begin with such an analysis, we first define the velocity error $\boldsymbol{e}_{\boldsymbol{u}}$, the pressure error e_p, and the temperature error e_t as follows:

$$\boldsymbol{e}_{\boldsymbol{u}} := \boldsymbol{u} - \boldsymbol{u}_{\mathscr{T}}, \quad e_p := p - p_{\mathscr{T}}, \quad e_t := t - t_{\mathscr{T}}. \tag{28}$$

5.1. **Reliability analysis: a Ritz projection of the errors.** To construct an a posteriori error estimator that provides an upper bound for the error, in energy-type norms, we will consider, on the basis of the ideas developed in [2], a Ritz projection of the residuals. To be precise, such a Ritz projection $(\boldsymbol{\Phi}, \psi, \varphi)$ is defined as the solution to the following problem: Find $(\boldsymbol{\Phi}, \psi, \varphi) \in \boldsymbol{H}^1_0(\Omega) \times L^2_0(\Omega) \times H^1_0(\Omega)$ such that

$$\begin{aligned} \int_\Omega \nabla \boldsymbol{\Phi} : \nabla \boldsymbol{v} + \int_\Omega \psi q + \int_\Omega \nabla \varphi \cdot \nabla w &= [\mathcal{A}(t; \boldsymbol{u}, \boldsymbol{v}) - \mathcal{A}(t_{\mathscr{T}}; \boldsymbol{u}_{\mathscr{T}}, \boldsymbol{v})] + [\mathcal{C}(\boldsymbol{u}; \boldsymbol{u}, \boldsymbol{v}) - \mathcal{C}(\boldsymbol{u}_{\mathscr{T}}; \boldsymbol{u}_{\mathscr{T}}, \boldsymbol{v})] \\ &\quad - \mathcal{B}(\boldsymbol{v}, e_p) - \mathcal{D}(e_t, \boldsymbol{v}) + \mathcal{B}(\boldsymbol{e}_{\boldsymbol{u}}, q) + [\mathscr{A}(t; t, w) - \mathscr{A}(t_{\mathscr{T}}; t_{\mathscr{T}}, w)] + [\mathscr{C}(\boldsymbol{u}; t, w) - \mathscr{C}(\boldsymbol{u}_{\mathscr{T}}; t_{\mathscr{T}}, w)], \end{aligned} \tag{29}$$

for all $\boldsymbol{v} \in \boldsymbol{H}^1_0(\Omega)$, $q \in L^2_0(\Omega)$, and $w \in H^1_0(\Omega)$. The existence and uniqueness of $(\boldsymbol{\Phi}, \psi, \varphi)$ follows from the continuity properties of the forms $\mathcal{A}$, $\mathcal{B}$, $\mathcal{C}$, $\mathcal{D}$, $\mathscr{A}$, and $\mathscr{C}$ and the Lax–Milgram Theorem.

We now prove that the sum of the energy norms of the velocity, pressure, and temperature errors can be bounded in terms of the the energy norm of the Ritz projection.

Theorem 2 (upper bound for the error)**.** *If ξ satisfies*

$$\left\{ \begin{array}{rcl} \kappa_{lip} \mathfrak{C}_\Omega \|\nabla t\|_{L^3(\Omega)} + \kappa_{lip} \mathfrak{C}_\Omega \|\nabla e_t\|_{L^3(\Omega)} + C_{D,\Omega} |\boldsymbol{e}_{\boldsymbol{u}}|_{\boldsymbol{H}^1(\Omega)} &\leq & \xi, \\ \varepsilon_{lip} \mathfrak{C}_\Omega \|\nabla \boldsymbol{u}\|_{\boldsymbol{L}^3(\Omega)} + \varepsilon_{lip} \mathfrak{C}_\Omega \|\nabla \boldsymbol{e}_{\boldsymbol{u}}\|_{\boldsymbol{L}^3(\Omega)} + C_{D,\Omega} \|\boldsymbol{g}\|_{\boldsymbol{L}^2(\Omega)} &\leq & \xi, \\ C_{D,\Omega} |\boldsymbol{e}_{\boldsymbol{u}}|_{\boldsymbol{H}^1(\Omega)} + C_{D,\Omega} |\boldsymbol{u}|_{\boldsymbol{H}^1(\Omega)} + C_{D,\Omega} |t|_{H^1(\Omega)} &\leq & 2\xi, \end{array} \right. \tag{30}$$

and

$$0 < \xi < \min \left\{ \kappa_1, \frac{\varepsilon_1 \kappa_1}{\varepsilon_1 + 3\kappa_1} \right\}, \tag{31}$$

then, there exists a positive constant C that does not depend neither on $(\boldsymbol{\Phi}, \varphi, \psi)$ nor $(\boldsymbol{u}, p, t)$ such that

$$|\boldsymbol{e}_{\boldsymbol{u}}|^2_{\boldsymbol{H}^1(\Omega)} + \|e_p\|^2_{L^2(\Omega)} + |e_t|^2_{H^1(\Omega)} \leq C \left(|\boldsymbol{\Phi}|^2_{\boldsymbol{H}^1(\Omega)} + \|\psi\|^2_{L^2(\Omega)} + |\varphi|^2_{H^1(\Omega)} \right). \tag{32}$$

Proof. We divide the proof in several steps.

Step 1. We begin by exploiting the fact that $\mathcal{A}$, $\mathcal{B}$, $\mathscr{A}$, and $\mathscr{C}$ are linear in the second and third component to write (29) as follows:

$$\begin{aligned} &\int_\Omega \nabla \boldsymbol{\Phi} : \nabla \boldsymbol{v} + \int_\Omega \psi q + \int_\Omega \nabla \varphi \cdot \nabla w \\ &\qquad = \left[\mathcal{A}(t; \boldsymbol{e}_{\boldsymbol{u}}, \boldsymbol{v}) + \{ (\mathcal{A}(t; \boldsymbol{u}, \boldsymbol{v}) - \mathcal{A}(t_{\mathscr{T}}; \boldsymbol{u}, \boldsymbol{v})) - (\mathcal{A}(t; \boldsymbol{e}_{\boldsymbol{u}}, \boldsymbol{v}) - \mathcal{A}(t_{\mathscr{T}}; \boldsymbol{e}_{\boldsymbol{u}}, \boldsymbol{v})) \} \right] \\ &\qquad + \left[\mathcal{C}(\boldsymbol{u}; \boldsymbol{e}_{\boldsymbol{u}}, \boldsymbol{v}) - \mathcal{C}(\boldsymbol{e}_{\boldsymbol{u}}; \boldsymbol{e}_{\boldsymbol{u}}, \boldsymbol{v}) + \mathcal{C}(\boldsymbol{e}_{\boldsymbol{u}}; \boldsymbol{u}, \boldsymbol{v}) \right] + \mathcal{B}(\boldsymbol{e}_{\boldsymbol{u}}, q) - \mathcal{B}(\boldsymbol{v}, e_p) - \mathcal{D}(e_t, \boldsymbol{v}) \\ &\qquad + \left[\mathscr{A}(t; e_t, w) + \{ (\mathscr{A}(t; t, w) - \mathscr{A}(t_{\mathscr{T}}; t, w)) - (\mathscr{A}(t; e_t, w) - \mathscr{A}(t_{\mathscr{T}}; e_t, w)) \} \right] \\ &\qquad + \left[\mathscr{C}(\boldsymbol{u}; e_t, w) - \mathscr{C}(\boldsymbol{e}_{\boldsymbol{u}}; e_t, w) + \mathscr{C}(\boldsymbol{e}_{\boldsymbol{u}}; t, w) \right]. \end{aligned} \tag{33}$$

Step 2. Set $(\boldsymbol{v}, q, w) = (\boldsymbol{0}, 0, e_t)$ and invoke (11), (12), and (13) to conclude that

$$\begin{aligned}\kappa_1 |e_t|^2_{H^1(\Omega)} &\leq \kappa_{lip}\mathfrak{C}_\Omega |e_t|^2_{H^1(\Omega)} \|\nabla t\|_{L^3(\Omega)} + \kappa_{lip}\mathfrak{C}_\Omega |e_t|^2_{H^1(\Omega)} \|\nabla e_t\|_{L^3(\Omega)} + C_{D,\Omega}|e_t|^2_{H^1(\Omega)}|\boldsymbol{e_u}|_{\boldsymbol{H}^1(\Omega)} \\ &\quad + C_{D,\Omega}|\boldsymbol{e_u}|_{\boldsymbol{H}^1(\Omega)}|t|_{H^1(\Omega)}|e_t|_{H^1(\Omega)} + |\varphi|_{H^1(\Omega)}|e_t|_{H^1(\Omega)} \\ &= |e_t|^2_{H^1(\Omega)} \left\{ \kappa_{lip}\mathfrak{C}_\Omega \|\nabla t\|_{L^3(\Omega)} + \kappa_{lip}\mathfrak{C}_\Omega \|\nabla e_t\|_{L^3(\Omega)} + C_{D,\Omega}|\boldsymbol{e_u}|_{\boldsymbol{H}^1(\Omega)} \right\} \\ &\quad + |e_t|_{H^1(\Omega)} \left\{ C_{D,\Omega}|t|_{H^1(\Omega)}|\boldsymbol{e_u}|_{\boldsymbol{H}^1(\Omega)} + |\varphi|_{H^1(\Omega)} \right\}.\end{aligned}$$

Notice that we have also used (16) which guarantees that $\mathscr{C}(\boldsymbol{u}; e_t, e_t) = 0$. Since ξ is such that (30) holds, we arrive at

$$(\kappa_1 - \xi)\, |e_t|_{\boldsymbol{H}^1(\Omega)} \leq C_{D,\Omega}|t|_{H^1(\Omega)}|\boldsymbol{e_u}|_{\boldsymbol{H}^1(\Omega)} + |\varphi|_{H^1(\Omega)}. \tag{34}$$

Notice that, since ξ satisfies (31), $\kappa_1 - \xi > 0$.

Step 3. Set $(\boldsymbol{v}, q, w) = (\boldsymbol{v}, 0, 0)$, with $\boldsymbol{v} \in \boldsymbol{H}^1_0(\Omega)$, in (29). This yields

$$\mathcal{B}(\boldsymbol{v}, e_p) = -\int_\Omega \nabla \boldsymbol{\Phi} : \nabla v + \mathcal{A}(t; \boldsymbol{u}, \boldsymbol{v}) - \mathcal{A}(t_{\mathscr{T}}; \boldsymbol{u}_{\mathscr{T}}, \boldsymbol{v}) + \mathcal{C}(\boldsymbol{u}; \boldsymbol{u}, \boldsymbol{v}) - \mathcal{C}(\boldsymbol{u}_{\mathscr{T}}; \boldsymbol{u}_{\mathscr{T}}, \boldsymbol{v}) - \mathcal{D}(e_t, \boldsymbol{v}).$$

Invoking the inf-sup condition (18) and utilizing that the right-hand side of (29) can be equivalently written as the right-hand side of (33), we can thus conclude that

$$\begin{aligned}\beta \|e_p\|_{L^2(\Omega)} &\leq \sup_{\boldsymbol{v} \in \boldsymbol{H}^1_0(\Omega)\setminus\{\boldsymbol{0}\}} \frac{|\mathcal{B}(\boldsymbol{v}, e_p)|}{|\boldsymbol{v}|_{\boldsymbol{H}^1_0(\Omega)}} \leq |\boldsymbol{\Phi}|_{\boldsymbol{H}^1(\Omega)} + \varepsilon_2 |\boldsymbol{e_u}|_{\boldsymbol{H}^1(\Omega)} + 2C_{D,\Omega}|\boldsymbol{u}|_{\boldsymbol{H}^1(\Omega)}|\boldsymbol{e_u}|_{\boldsymbol{H}^1(\Omega)} \\ &\quad + C_{D,\Omega}|\boldsymbol{e_u}|^2_{\boldsymbol{H}^1(\Omega)} + |e_t|_{H^1(\Omega)} \left\{ \varepsilon_{lip}\mathfrak{C}_\Omega \|\nabla \boldsymbol{u}\|_{\boldsymbol{L}^3(\Omega)} + \varepsilon_{lip}\mathfrak{C}_\Omega \|\nabla \boldsymbol{e_u}\|_{\boldsymbol{L}^3(\Omega)} + C_{D,\Omega}\|\boldsymbol{g}\|_{\boldsymbol{L}^2(\Omega)} \right\}. \end{aligned} \tag{35}$$

By using (30), it then follows that

$$\beta \|e_p\|_{L^2(\Omega)} \leq |\boldsymbol{\Phi}|_{\boldsymbol{H}^1(\Omega)} + |\boldsymbol{e_u}|_{\boldsymbol{H}^1(\Omega)} \left\{ \varepsilon_2 + 2C_{D,\Omega}|\boldsymbol{u}|_{\boldsymbol{H}^1(\Omega)} + C_{D,\Omega}|\boldsymbol{e_u}|_{\boldsymbol{H}^1(\Omega)} \right\} + |e_t|_{H^1(\Omega)}\xi.$$

We thus invoke (34) and conclude that

$$\begin{aligned}\beta \|e_p\|_{L^2(\Omega)} &\leq |\boldsymbol{\Phi}|_{\boldsymbol{H}^1(\Omega)} + |\boldsymbol{e_u}|_{\boldsymbol{H}^1(\Omega)} \left\{ \varepsilon_2 + 2C_{D,\Omega}|\boldsymbol{u}|_{\boldsymbol{H}^1(\Omega)} + C_{D,\Omega}|\boldsymbol{e_u}|_{\boldsymbol{H}^1(\Omega)} \right\} \\ &\quad + \xi(\kappa_1 - \xi)^{-1} \left\{ C_{D,\Omega}|t|_{H^1(\Omega)}|\boldsymbol{e_u}|_{\boldsymbol{H}^1(\Omega)} + |\varphi|_{H^1(\Omega)} \right\}. \end{aligned} \tag{36}$$

Step 4. Set $(\boldsymbol{v}, q, w) = (\boldsymbol{e_u}, -e_p, 0)$ in (33) and invoke similar arguments to the ones used in the previous step to conclude that

$$\begin{aligned}&\varepsilon_1 |\boldsymbol{e_u}|^2_{\boldsymbol{H}^1(\Omega)} \\ &\leq |\boldsymbol{\Phi}|_{\boldsymbol{H}^1(\Omega)}|\boldsymbol{e_u}|_{\boldsymbol{H}^1(\Omega)} + \varepsilon_{lip}\mathfrak{C}_\Omega |e_t|_{H^1(\Omega)} \|\nabla \boldsymbol{u}\|_{\boldsymbol{L}^3(\Omega)}|\boldsymbol{e_u}|_{\boldsymbol{H}^1(\Omega)} + \varepsilon_{lip}\mathfrak{C}_\Omega |e_t|_{H^1(\Omega)} \|\nabla \boldsymbol{e_u}\|_{\boldsymbol{L}^3(\Omega)}|\boldsymbol{e_u}|_{\boldsymbol{H}^1(\Omega)} \\ &\quad + C_{D,\Omega}|\boldsymbol{e_u}|^3_{\boldsymbol{H}^1(\Omega)} + C_{D,\Omega}|\boldsymbol{e_u}|^2_{\boldsymbol{H}^1(\Omega)}|\boldsymbol{u}|_{\boldsymbol{H}^1(\Omega)} + C_{D,\Omega}\|\boldsymbol{g}\|_{\boldsymbol{L}^2(\Omega)}|e_t|_{H^1(\Omega)}|\boldsymbol{e_u}|_{\boldsymbol{H}^1(\Omega)} + \|\psi\|_{L^2(\Omega)}\|e_p\|_{L^2(\Omega)} \\ &\leq |\boldsymbol{e_u}|^2_{\boldsymbol{H}^1(\Omega)} \left\{ C_{D,\Omega}|\boldsymbol{e_u}|_{\boldsymbol{H}^1(\Omega)} + C_{D,\Omega}|\boldsymbol{u}|_{\boldsymbol{H}^1(\Omega)} \right\} + |\boldsymbol{\Phi}|_{\boldsymbol{H}^1(\Omega)}|\boldsymbol{e_u}|_{\boldsymbol{H}^1(\Omega)} \\ &\quad + |e_t|_{H^1(\Omega)}|\boldsymbol{e_u}|_{\boldsymbol{H}^1(\Omega)} \left\{ \varepsilon_{lip}\mathfrak{C}_\Omega \|\nabla \boldsymbol{u}\|_{\boldsymbol{L}^3(\Omega)} + \varepsilon_{lip}\mathfrak{C}_\Omega \|\nabla \boldsymbol{e_u}\|_{\boldsymbol{L}^3(\Omega)} + C_{D,\Omega}\|\boldsymbol{g}\|_{\boldsymbol{L}^2(\Omega)} \right\} + \|\psi\|_{L^2(\Omega)}\|e_p\|_{L^2(\Omega)} \\ &\leq 2\xi |\boldsymbol{e_u}|^2_{\boldsymbol{H}^1(\Omega)} + |\boldsymbol{\Phi}|_{\boldsymbol{H}^1(\Omega)}|\boldsymbol{e_u}|_{\boldsymbol{H}^1(\Omega)} + \xi |e_t|_{H^1(\Omega)}|\boldsymbol{e_u}|_{H^1(\Omega)} + \|\psi\|_{L^2(\Omega)}\|e_p\|_{L^2(\Omega)}, \end{aligned}$$

where, to obtain the last inequality, we have used (30). We thus utilize the estimates for $|e_t|_{H^1(\Omega)}$ and $\|e_p\|_{L^2(\Omega)}$ obtained in (34) and (36), respectively to conclude that

$$\begin{aligned}&\varepsilon_1 |\boldsymbol{e_u}|^2_{\boldsymbol{H}^1(\Omega)} \\ &\leq |\boldsymbol{e_u}|^2_{\boldsymbol{H}^1(\Omega)} \left\{ 2\xi + \frac{\xi}{\kappa_1 - \xi} C_{D,\Omega}|t|_{H^1(\Omega)} \right\} + \frac{1}{\beta}\|\psi\|_{L^2(\Omega)}|\boldsymbol{\Phi}|_{\boldsymbol{H}^1(\Omega)} \\ &\quad + \frac{\xi}{\kappa_1 - \xi}\frac{1}{\beta}\|\psi\|_{L^2(\Omega)}|\varphi|_{H^1(\Omega)} + |\boldsymbol{e_u}|_{\boldsymbol{H}^1(\Omega)} \Bigg\{ |\boldsymbol{\Phi}|_{\boldsymbol{H}^1(\Omega)} + \frac{\xi}{\kappa_1 - \xi}|\varphi|_{H^1(\Omega)} \\ &\quad + \frac{1}{\beta}\|\psi\|_{L^2(\Omega)} \left[\frac{\xi}{\kappa_1 - \xi} C_{D,\Omega}|t|_{H^1(\Omega)} + \varepsilon_2 + 2C_{D,\Omega}|\boldsymbol{u}|_{\boldsymbol{H}^1(\Omega)} + C_{D,\Omega}|\boldsymbol{e_u}|_{\boldsymbol{H}^1(\Omega)} \right] \Bigg\}. \end{aligned}$$

We invoke (30), which guarantees that $C_{D,\Omega}|t|_{H^1(\Omega)} \leq 2\xi$ and that $C_{D,\Omega}|\boldsymbol{u}|_{\boldsymbol{H}^1(\Omega)} + C_{D,\Omega}|\boldsymbol{e_u}|_{\boldsymbol{H}^1(\Omega)} \leq 2\xi$ to conclude that

$$\varepsilon_1|\boldsymbol{e_u}|^2_{\boldsymbol{H}^1(\Omega)} \leq |\boldsymbol{e_u}|^2_{\boldsymbol{H}^1(\Omega)}\left\{2\xi + \frac{2\xi^2}{\kappa_1-\xi}\right\} + \frac{1}{\beta}\|\psi\|_{L^2(\Omega)}|\boldsymbol{\Phi}|_{\boldsymbol{H}^1(\Omega)} + \frac{1}{\beta}\frac{\xi}{\kappa_1-\xi}\|\psi\|_{L^2(\Omega)}|\varphi|_{H^1(\Omega)}$$
$$+ |\boldsymbol{e_u}|_{\boldsymbol{H}^1(\Omega)}\left\{|\boldsymbol{\Phi}|_{\boldsymbol{H}^1(\Omega)} + \frac{\xi}{\kappa_1-\xi}|\varphi|_{H^1(\Omega)} + \frac{1}{\beta}\|\psi\|_{L^2(\Omega)}\left[\frac{2\xi^2}{\kappa_1-\xi} + \varepsilon_2 + 4\xi\right]\right\}.$$

Denote $\delta = 2\xi + \frac{2\xi^2}{\kappa_1-\xi} = \frac{2\xi\kappa_1}{\kappa_1-\xi}$. Invoke the basic estimate $ab \leq (\delta/2)a^2 + (1/2\delta)b^2$ to conclude that

$$\left(\varepsilon_1 - \delta - \frac{\delta}{2}\right)|\boldsymbol{e_u}|^2_{\boldsymbol{H}^1(\Omega)} \leq C\left(|\boldsymbol{\Phi}|^2_{\boldsymbol{H}^1(\Omega)} + |\varphi|^2_{H^1(\Omega)} + \|\psi\|^2_{L^2(\Omega)}\right), \tag{37}$$

with a constant C that does not depend neither on $(\boldsymbol{\Phi}, \varphi, \psi)$ nor $(\boldsymbol{u}, p, t)$. Notice that, in view of (31), we have

$$\varepsilon_1 - \delta - \frac{\delta}{2} = \varepsilon_1 - \frac{3}{2}\delta = \frac{1}{\kappa_1-\xi}\left(\varepsilon_1(\kappa_1-\xi) - 3\xi\kappa_1\right) > 0.$$

We can finally conclude that

$$|\boldsymbol{e_u}|^2_{\boldsymbol{H}^1(\Omega)} \leq C\left(|\boldsymbol{\Phi}|^2_{\boldsymbol{H}^1(\Omega)} + |\varphi|^2_{H^1(\Omega)} + \|\psi\|^2_{L^2(\Omega)}\right).$$

Step 5. The desired estimate (32) follows from the previous estimate combined with (34) and (36). □

Remark (global reliability and local efficiency estimates). In [2], the authors prove, for the Stokes and Ossen equations, that the energy norm of the error is *equivalent* to the energy norm of the Ritz projection of the residuals. On the basis of such a result, a posteriori error estimates were derived: global reliability and local efficiency estimates. In our case, we will only consider the upper bound (32) for the error. From this bound a reliability analysis can be obtained; see Theorems 3, 4, and 5. In section 5.4, we will derive local efficiency estimates on the basis of standard bubble functions arguments.

5.2. **Reliability analysis: a residual-type error estimation.** In Theorem 2 we proved that the total error is bounded by the energy norm of the Ritz projection of the residuals. In this section we focus on bounding each term appearing in the right-hand side of (32). We proceed on the basis of three steps.

Step 1: Set $(\boldsymbol{v}, q, w) = (\boldsymbol{v}, 0, 0)$ in (29). Let us denote by $\mathcal{I}_{\mathscr{T}}$ the Clément-type interpolation operator of [40, equation 3.3]. Utilizing (8) and an integration by parts formula we conclude, for $\boldsymbol{v} \in \boldsymbol{H}^1_0(\Omega)$, that

$$\int_\Omega \nabla\boldsymbol{\Phi} : \nabla\boldsymbol{v} = \sum_{K\in\mathscr{T}}\left(\int_K \boldsymbol{R}_K(\boldsymbol{v} - \mathcal{I}_{\mathscr{T}}(\boldsymbol{v})) - \frac{1}{2}\sum_{\gamma\in\mathcal{F}_K}\int_\gamma \boldsymbol{J}_\gamma(\boldsymbol{v} - \mathcal{I}_{\mathscr{T}}(\boldsymbol{v}))\right) - \mathcal{S}_F(\boldsymbol{u}_{\mathscr{T}}, \mathcal{I}_{\mathscr{T}}(\boldsymbol{v})), \tag{38}$$

where

$$\left\{\begin{array}{rcl} \boldsymbol{R}_K & := & \boldsymbol{f} + \mathbf{div}(\varepsilon(t_{\mathscr{T}})\nabla\boldsymbol{u}_{\mathscr{T}})_{|K} - \boldsymbol{u}_{\mathscr{T}|K}\nabla\boldsymbol{u}_{\mathscr{T}|K} - \nabla p_{\mathscr{T}|K} + \boldsymbol{g}t_{\mathscr{T}|K}, \\ \boldsymbol{J}_\gamma & := & [\![(\varepsilon(t_{\mathscr{T}})\nabla\boldsymbol{u}_{\mathscr{T}} - p_{\mathscr{T}}\mathbf{I})\cdot\boldsymbol{n}_\gamma]\!]. \end{array}\right. \tag{39}$$

The term $\boldsymbol{J}_\gamma$ is defined as follows: for $\gamma \in \mathcal{F}_K \cap \mathcal{F}_{K'}$ with $K \neq K'$ and $K, K' \in \mathscr{T}$,

$$\boldsymbol{J}_\gamma = [\![(\varepsilon(t_{\mathscr{T}})\nabla\boldsymbol{u}_{\mathscr{T}} - p_{\mathscr{T}}\mathbf{I})\cdot\boldsymbol{n}_\gamma]\!] = (\varepsilon(t_{\mathscr{T}})_{|K}\nabla\boldsymbol{u}_{\mathscr{T}|K} - p_{\mathscr{T}|K}\mathbf{I})\cdot\boldsymbol{n}^K_\gamma + (\varepsilon(t_{\mathscr{T}})_{|K'}\nabla\boldsymbol{u}_{\mathscr{T}|K'} - p_{\mathscr{T}|K'}\mathbf{I})\cdot\boldsymbol{n}^{K'}_\gamma.$$

Define

$$\vartheta^2_F := \sum_{K\in\mathscr{T}}\vartheta^2_{K,F}, \qquad \vartheta^2_{K,F} := h^2_K\|\boldsymbol{R}_K\|^2_{\boldsymbol{L}^2(K)} + \sum_{\gamma\in\mathcal{F}_K\cap\mathcal{F}_I} h_K\|\boldsymbol{J}_\gamma\|^2_{\boldsymbol{L}^2(\gamma)}. \tag{40}$$

We invoke [40, Lemma 3.3] and the fact that $\int_\Omega \nabla\boldsymbol{\Phi} : \nabla\boldsymbol{v}$ is coercive on $\boldsymbol{H}^1_0(\Omega)$ to conclude that

$$|\boldsymbol{\Phi}|^2_{\boldsymbol{H}^1(\Omega)} \leq C\left(\vartheta^2_F + \left[\sup_{\boldsymbol{v}\in\boldsymbol{H}^1_0(\Omega)\setminus\{\mathbf{0}\}}\frac{\mathcal{S}_F(\boldsymbol{u}_{\mathscr{T}}, \mathcal{I}_{\mathscr{T}}(\boldsymbol{v}))}{|\boldsymbol{v}|_{\boldsymbol{H}^1(\Omega)}}\right]^2\right). \tag{41}$$

Step 2: Set $(\boldsymbol{v}, q, w) = (\mathbf{0}, \psi, 0)$ in (29). This yields

$$\|\psi\|^2_{L^2(\Omega)} = \mathcal{B}(\boldsymbol{e_u}, \psi) = -\mathcal{B}(\boldsymbol{u}_{\mathscr{T}}, \psi) \leq \|\nabla\cdot\boldsymbol{u}_{\mathscr{T}}\|_{L^2(\Omega)}\|\psi\|_{L^2(\Omega)},$$

upon using the definition of the bilinear form $\mathcal{B}$, the fact that $\boldsymbol{u} \in \boldsymbol{X}(\Omega)$, and the Cauchy–Schwarz inequality. The previous inequality immediately yields

$$\|\psi\|^2_{L^2(\Omega)} \leq \|\nabla\cdot\boldsymbol{u}_{\mathscr{T}}\|^2_{L^2(\Omega)}.$$

Step 3: Set $(\boldsymbol{v}, q, w) = (\boldsymbol{0}, 0, w)$ in (29). Following similar arguments to the ones developed in Step 1, we arrive at that the following error-type equation, which holds for all $w \in H_0^1(\Omega)$,

$$\int_\Omega \nabla\varphi \cdot \nabla w = \sum_{K\in\mathscr{T}} \left(\int_K R_K(w - \mathcal{I}_\mathscr{T}(w)) - \frac{1}{2} \sum_{\gamma\in\mathcal{F}_K} \int_\gamma J_\gamma(w - \mathcal{I}_\mathscr{T}(w)) \right) - \mathcal{S}_T(t_\mathscr{T}, \mathcal{I}_\mathscr{T}(w)), \tag{42}$$

where

$$\left\{ \begin{array}{rcl} R_K & := & h + \operatorname{div}(\kappa(t_\mathscr{T})\nabla t_\mathscr{T})_{|K} - \boldsymbol{u}_{\mathscr{T}|K} \cdot \nabla t_{\mathscr{T}|K}, \\ J_\gamma & := & [\![\kappa(t_\mathscr{T})\nabla t_\mathscr{T} \cdot \boldsymbol{n}_\gamma]\!]. \end{array} \right. \tag{43}$$

The jump term J_γ is defined as the one presented in (39).

Define

$$\vartheta_T^2 := \sum_{K\in\mathscr{T}} \vartheta_{K,T}^2, \qquad \vartheta_{K,T}^2 := h_K^2 \|R_K\|_{L^2(K)}^2 + \sum_{\gamma\in\mathcal{F}_K\cap\mathcal{F}_I} h_K \|J_\gamma\|_{L^2(\gamma)}^2. \tag{44}$$

Applying the same arguments that lead to (45) we conclude that

$$|\varphi|_{H^1(\Omega)}^2 \leq C \left(\vartheta_T^2 + \left[\sup_{w\in H_0^1(\Omega)\setminus\{0\}} \frac{\mathcal{S}_T(t_\mathscr{T}, \mathcal{I}_\mathscr{T}(w))}{|w|_{H^1(\Omega)}} \right]^2 \right). \tag{45}$$

Define the a posteriori error estimator ϑ as

$$\vartheta^2 := \sum_{K\in\mathscr{T}} \vartheta_K^2,$$

where the error indicator ϑ_K is defined by

$$\begin{aligned} \vartheta_K^2 := h_K^2 \left(\|\boldsymbol{R}_K\|_{\boldsymbol{L}^2(K)}^2 + \|R_K\|_{L^2(K)}^2 \right) + \|\nabla\cdot\boldsymbol{u}_\mathscr{T}\|_{L^2(K)}^2 \\ + \sum_{\gamma\in\mathcal{F}_K\cap\mathcal{F}_I} h_K \left(\|\boldsymbol{J}_\gamma\|_{\boldsymbol{L}^2(\gamma)}^2 + \|J_\gamma\|_{L^2(\gamma)}^2 \right). \end{aligned} \tag{46}$$

With this definition at hand, we present the following global reliability result.

Theorem 3 (global reliability)**.** *Let $(\boldsymbol{u}, p, t)$ be the solution to* (8) *and $(\boldsymbol{u}_\mathscr{T}, p_\mathscr{T}, t_\mathscr{T})$ its finite element approximation given as the solution to* (25)*. If* (30) *holds then, there exist a positive constant C such that*

$$\begin{aligned} |\boldsymbol{e}_{\boldsymbol{u}}|_{\boldsymbol{H}^1(\Omega)}^2 + \|e_p\|_{L^2(\Omega)}^2 + |e_t|_{H^1(\Omega)}^2 \\ \leq C \left(\vartheta^2 + \left[\sup_{\boldsymbol{v}\in\boldsymbol{H}_0^1(\Omega)\setminus\{\boldsymbol{0}\}} \frac{\mathcal{S}_F(\boldsymbol{u}_\mathscr{T}, \mathcal{I}_\mathscr{T}(\boldsymbol{v}))}{|\boldsymbol{v}|_{\boldsymbol{H}^1(\Omega)}} \right]^2 + \left[\sup_{w\in H_0^1(\Omega)\setminus\{0\}} \frac{\mathcal{S}_T(t_\mathscr{T}, \mathcal{I}_\mathscr{T}(w))}{|w|_{H^1(\Omega)}} \right]^2 \right). \end{aligned} \tag{47}$$

Proof. The desired result follows from combining the estimates obtained in Steps 1, 2, and 3, together with the result of Theorem 2. □

5.3. **Elections for stabilized terms: a final upper bound.** In this section, we consider some particular elections of stabilization terms $\mathcal{S}_F$ and $\mathcal{S}_T$ and estimate the so-called consistency errors that appear in the right-hand side of the a posteriori error estimate (47) thereby obtaining a final upper bound for the error in terms of computable quantities.

For the fluid flow, we consider a grad-div type of stabilization term, that was first introduced, for a Stokes problem, in [25]:

$$\mathcal{S}_F(\boldsymbol{v}_\mathscr{T}, \boldsymbol{w}_\mathscr{T}) = \tau \sum_{K\in\mathscr{T}} h_K \int_K \nabla\cdot\boldsymbol{v}_\mathscr{T} \nabla\cdot\boldsymbol{w}_\mathscr{T}, \qquad \boldsymbol{v}_\mathscr{T}, \boldsymbol{w}_\mathscr{T} \in \boldsymbol{V}(\mathscr{T}).$$

The positive parameter τ is the so-called stabilization constant. We stress that the election $\mathcal{S}_F \equiv 0$ is also valid.

Second, for for the temperature equation, we can consider the following election [15]:

$$\mathcal{S}_T(v_\mathscr{T}, w_\mathscr{T}) = \tilde{\tau} \sum_{\gamma\in\mathcal{F}_I} h_\gamma^2 \int_\gamma [\![\nabla v_\mathscr{T} \cdot \boldsymbol{n}_\gamma]\!][\![\nabla w_\mathscr{T} \cdot \boldsymbol{n}_\gamma]\!], \qquad v_\mathscr{T}, w_\mathscr{T} \in V(\mathscr{T}).$$

where $\tilde{\tau} > 0$ corresponds to a stabilization constant. We mention that the election $\mathcal{S}_T \equiv 0$ is valid as well.

With these ingredients at hand, we are ready to state and prove the following result.

Theorem 4 (final global reliability)**.** *Let $(\boldsymbol{u},p,t)$ be the solution to* (8) *and $(\boldsymbol{u}_{\mathscr{T}},p_{\mathscr{T}},t_{\mathscr{T}})$ its finite element approximation given as the solution to* (25)*. If* (30) *holds, then there exists a positive constant C such that*

$$|\boldsymbol{e}_{\boldsymbol{u}}|^2_{\boldsymbol{H}^1(\Omega)}+\|e_p\|^2_{L^2}+|e_t|^2_{H^1(\Omega)}\leq C\eta^2,$$

where the error estimator η is defined as

$$\eta^2:=\sum_{K\in\mathscr{T}}\eta_K^2,$$

with the local indicators η_K being defined as

$$\eta_K^2:=h_K^2\left(\|\boldsymbol{R}_K\|^2_{\boldsymbol{L}^2(K)}+\|R_K\|^2_{L^2(K)}\right)+(1+\tau^2h_K^2)\|\nabla\cdot\boldsymbol{u}_{\mathscr{T}}\|^2_{L^2(K)}+\sum_{\gamma\in\mathcal{F}_K\cap\mathcal{F}_I}h_K\left(\|\boldsymbol{J}_\gamma\|^2_{\boldsymbol{L}^2(\gamma)}+\left(1+\tilde{\tau}h_K^3\right)\|J_\gamma\|^2_{L^2(\gamma)}\right).\quad(48)$$

Proof. In view of the result of Theorem 3 it suffices to control the consistency terms $\mathcal{S}_F$ and $\mathcal{S}_T$. We begin by controlling the term $\mathcal{S}_F$. In fact, we have that

$$\sup_{\substack{\boldsymbol{v}\in\boldsymbol{H}^1_0(\Omega)\\ \boldsymbol{v}\neq\boldsymbol{0}}}\frac{\mathcal{S}_F(\boldsymbol{u}_{\mathscr{T}},\mathcal{I}_{\mathscr{T}}(\boldsymbol{v}))}{|\boldsymbol{v}|_{\boldsymbol{H}^1(\Omega)}}=\sup_{\substack{\boldsymbol{v}\in\boldsymbol{H}^1_0(\Omega)\\ \boldsymbol{v}\neq\boldsymbol{0}}}\frac{\displaystyle\sum_{K\in\mathscr{T}}\tau h_K\int_K\nabla\cdot\boldsymbol{u}_{\mathscr{T}}\nabla\cdot\mathcal{I}_{\mathscr{T}}(\boldsymbol{v})}{|\boldsymbol{v}|_{\boldsymbol{H}^1(\Omega)}}\leq C\left(\sum_{K\in\mathscr{T}}\tau^2h_K^2\|\nabla\cdot\boldsymbol{u}_K\|^2_{L^2(K)}\right)^{1/2},$$

where we have used the local stability of the interpolation operator $\mathcal{I}_{\mathscr{T}}$ [40, Lemma 3.3], the finite overlapping property of stars, and a Cauchy–Schwarz inequality.

We now bound the consistency term related with the temperature equation. Let $\gamma\in\mathcal{F}_K\cap\mathcal{F}_{K'}$ with $K\neq K'$ and $K,K'\in\mathscr{T}$. We begin with the following basic estimate, which holds for $w_{\mathscr{T}}\in V(\mathscr{T})$:

$$\|[\![\nabla w_{\mathscr{T}}\cdot\boldsymbol{n}_\gamma]\!]\|^2_{L^2(\gamma)}\leq C\sum_{K\in\Omega_\gamma}h_K^{-1}\|\nabla w_{\mathscr{T}}\|^2_{L^2(K)}.$$

Consequently,

$$\begin{aligned}&\sup_{w\in H^1_0(\Omega)\setminus\{0\}}\frac{\mathcal{S}_T(t_{\mathscr{T}},\mathcal{I}_{\mathscr{T}}(w))}{|w|_{H^1(\Omega)}}\\&\leq\sup_{w\in H^1_0(\Omega)\setminus\{0\}}\frac{1}{|w|_{H^1(\Omega)}}\left(\sum_{\gamma\in\mathcal{F}_I}\tilde{\tau}^2h_\gamma^4\|[\![\nabla t_{\mathscr{T}}\cdot\boldsymbol{n}_\gamma]\!]\|^2_{L^2(\gamma)}\right)^{1/2}\left(\sum_{\gamma\in\mathcal{F}_I}\|[\![\nabla\mathcal{I}_{\mathscr{T}}(w)\cdot\boldsymbol{n}_\gamma]\!]\|^2_{L^2(\gamma)}\right)^{1/2}\\&\leq C\sup_{w\in H^1_0(\Omega)\setminus\{0\}}\frac{1}{|w|_{H^1(\Omega)}}\left(\sum_{\gamma\in\mathcal{F}_I}\tilde{\tau}^2h_\gamma^3\|[\![\nabla t_{\mathscr{T}}\cdot\boldsymbol{n}_\gamma]\!]\|^2_{L^2(\gamma)}\right)^{1/2}\left(\sum_{\gamma\in\mathcal{F}_I}\sum_{K\in\Omega_\gamma}\|\nabla\mathcal{I}_{\mathscr{T}}(w)\|^2_{L^2(K)}\right)^{1/2}.\end{aligned}$$

We now invoke the finite overlapping property of stars to conclude that

$$\sup_{w\in H^1_0(\Omega)\setminus\{0\}}\frac{S_T(t_{\mathscr{T}},\mathcal{I}_{\mathscr{T}}(w))}{|w|_{H^1(\Omega)}}\leq C\left(\sum_{\gamma\in\mathcal{F}_I}\tilde{\tau}^2h_\gamma^3\|[\![\nabla t_{\mathscr{T}}\cdot\boldsymbol{n}_\gamma]\!]\|^2_{L^2(\gamma)}\right)^{1/2}.$$

This concludes the proof. □

We now focus in providing a posteriori error estimates for when the **SFEM2** technique is used. In order to present the following result and, since, in this case, the velocity field is a nonconforming function, we introduce the notation:

$$\boldsymbol{e}_{\mathfrak{L}}:=\boldsymbol{u}-\mathfrak{L}(\boldsymbol{u}_{\mathscr{T}},p_{\mathscr{T}}),\qquad|\boldsymbol{v}|^2_{\boldsymbol{H}^1(\mathscr{T})}:=\sum_{K\in\mathscr{T}}|\boldsymbol{v}|^2_{\boldsymbol{H}^1(K)}.\quad(49)$$

We present the following a posteriori error estimate.

Theorem 5 (final global reliability)**.** *Let $(\boldsymbol{u},p,t)$ be the solution to problem* (8) *and $(\mathfrak{L}(\boldsymbol{u}_{\mathscr{T}},p_{\mathscr{T}}),p_{\mathscr{T}},t_{\mathscr{T}})$ its nonconforming finite element approximation which enriches the velocity field as described in* (26)*. If* (30) *holds then, there exists a positive constant C such that*

$$|\boldsymbol{e}_{\mathfrak{L}}|^2_{\boldsymbol{H}^1(\mathscr{T})}+\|e_p\|^2_{L^2}+|e_t|^2_{H^1(\Omega)}\leq C\Theta^2,$$

where the error estimator Θ *is defined as*

$$\Theta^2 := \sum_{K\in\mathscr{T}} \Theta_K^2,$$

with the local indicators Θ_K *being defined as*

$$\Theta_K^2 := h_K^2 \left(\|\boldsymbol{R}_K\|^2_{\boldsymbol{L}^2(K)} + \|R_K\|^2_{L^2(K)} \right) + (1+\tau^2 h_K^2)\|\nabla\cdot\boldsymbol{u}_{\mathscr{T}}\|^2_{L^2(K)} + \sum_{\gamma\in\mathcal{F}_K\cap\mathcal{F}_I} h_K \left(\|\boldsymbol{J}_\gamma\|^2_{\boldsymbol{L}^2(\gamma)} + \left(1+\tilde{\tau}h_K^3\right)\|J_\gamma\|^2_{L^2(\gamma)} + \|[\![p_{\mathscr{T}}]\!]\|^2_{L^2(\gamma)} \right). \quad (50)$$

Proof. In view of [5, Theorem 4], that is still valid in our framework (see also [12, Lemma 3.9]), we have that

$$|\boldsymbol{e}_{\mathfrak{L}}|^2_{\boldsymbol{H}^1(\mathscr{T})} \leq C \left(|\boldsymbol{e}_{\boldsymbol{u}}|^2_{\boldsymbol{H}^1(\Omega)} + \sum_{\gamma\in\mathcal{F}_I} \frac{h_\gamma}{12} \|[\![p_{\mathscr{T}}]\!]\|^2_{L^2(\gamma)} \right).$$

The desired estimate thus follows from invoking the result of Theorem 4. □

5.4. **Local efficiency analysis.** We now proceed to investigate the local efficiency properties of the devised a posteriori error estimators on the basis of standard bubble function arguments [3, 41]. Before proceeding with such analysis, we introduce the following notation: For an edge, triangle or tetrahedron G, let $\mathcal{V}(G)$ be the set of vertices of G. With this notation at hand, we introduce element and edge bubble functions as follows. Let $K\in\mathscr{T}$ and $\gamma\in\mathcal{F}_I$. We define

$$\beta_K := (d+1)^{d+1} \prod_{\mathrm{v}\in\mathcal{V}(K)} \lambda_{\mathrm{v}|K}, \quad \beta_{\gamma|K} := d^d \prod_{\mathrm{v}\in\mathcal{V}(\gamma)} \lambda_{\mathrm{v}|K} \quad \text{with} \quad K\in\Omega_\gamma. \quad (51)$$

The following estimates will be frequently used in what follows: If $v_{\mathscr{T}}\in V(\mathscr{T})$, then [3, 41]

$$C\|v_{\mathscr{T}}\|^2_{L^2(K)} \leq \int_K \beta_K v_{\mathscr{T}}^2 \leq C\|v_{\mathscr{T}}\|_{L^2(K)}, \quad \|\beta_K v_{\mathscr{T}}\|_{L^2(K)} + h_K|\beta_K v_{\mathscr{T}}|_{H^1(K)} \leq C\|v_{\mathscr{T}}\|_{L^2(K)}. \quad (52)$$

and

$$C\|v_{\mathscr{T}}\|^2_{L^2(\gamma)} \leq \int_\gamma \beta_\gamma v_{\mathscr{T}}^2 \leq C\|v_{\mathscr{T}}\|_{L^2(\gamma)}, \quad h_K^{-\frac{1}{2}}\|\beta_\gamma v_{\mathscr{T}}\|_{L^2(K)} + h_K^{\frac{1}{2}}|\beta_\gamma v_{\mathscr{T}}|_{H^1(K)} \leq C\|v_{\mathscr{T}}\|_{L^2(\gamma)}, \quad (53)$$

where $K\in\Omega_\gamma$. We consider the natural extensions of (52) and (53) for the vector-value case.

Theorem 6 (local efficiency)**.** *Let* $(\boldsymbol{u},p,t)$ *be the solution to problem* (8) *and* $(\boldsymbol{u}_{\mathscr{T}},p_{\mathscr{T}},t_{\mathscr{T}})$ *its finite element approximation given as the solution to* (25)*. If* (30) *holds, then the local error indicator* η_K*, defined in* (48)*, satisfies, for every* $K\in\mathscr{T}$*,*

$$\eta_K^2 \leq C \sum_{\gamma\in\mathcal{F}_K} \sum_{K'\in\Omega_\gamma} \left(\|\boldsymbol{e}_{\boldsymbol{u}}\|^2_{\boldsymbol{H}^1(K')} + \|e_p\|^2_{L^2(K')} + \|e_t\|^2_{H^1(K')} + h^2_{K'} \left(\|\mathbf{osc}_{K'}\|^2_{\boldsymbol{L}^2(K')} + \|\mathrm{osc}_{K'}\|^2_{L^2(K')} \right) \right).$$

Proof. We examine each of the contributions of η_K separately. We proceed in three steps:

Step 1: For $K\in\mathscr{T}$, we define the following residuals and oscillation terms:

$$\begin{cases} \hat{\boldsymbol{R}}_K &:= \boldsymbol{\Pi}_{K,1}(\boldsymbol{f}) + \mathbf{div}(\varepsilon(t_{\mathscr{T}})\nabla\boldsymbol{u}_{\mathscr{T}|K}) - \boldsymbol{u}_{\mathscr{T}}\nabla\boldsymbol{u}_{\mathscr{T}} - \nabla p_{\mathscr{T}|K} + \boldsymbol{\Pi}_{K,1}(\boldsymbol{g}t_{\mathscr{T}|K}), \\ \mathbf{osc}_K &:= \boldsymbol{f} - \boldsymbol{\Pi}_{K,1}(\boldsymbol{f}) + \boldsymbol{g}t_{\mathscr{T}} - \boldsymbol{\Pi}_{K,1}(\boldsymbol{g}t_{\mathscr{T}|K}). \end{cases} \quad (54)$$

Since $(\boldsymbol{u},p,t)$ solves (8), the definition of the forms $\mathcal{A}$, $\mathcal{B}$, $\mathcal{C}$, and $\mathcal{D}$ combined with an integration by parts formula allow us to conclude the following error equation, which holds for any $\boldsymbol{v}\in\boldsymbol{H}^1_0(\Omega)$:

$$\sum_{K\in\mathscr{T}} \int_K \hat{\boldsymbol{R}}_K\boldsymbol{v} - \sum_{\gamma\in\mathcal{F}_I} \int_\gamma \boldsymbol{J}_\gamma\boldsymbol{v} = [\mathcal{A}(t;\boldsymbol{u},\boldsymbol{v}) - \mathcal{A}(t_{\mathscr{T}};\boldsymbol{u}_{\mathscr{T}},\boldsymbol{v})] + [\mathcal{C}(\boldsymbol{u};\boldsymbol{u},\boldsymbol{v}) - \mathcal{C}(\boldsymbol{u}_{\mathscr{T}};\boldsymbol{u}_{\mathscr{T}},\boldsymbol{v})] - \mathcal{B}(\boldsymbol{v},e_p) - \mathcal{D}(e_t,\boldsymbol{v}) - \sum_{K\in\mathscr{T}} \int_K \mathbf{osc}_K\boldsymbol{v}. \quad (55)$$

We recall that $\boldsymbol{J}_\gamma$ is defined as in (39). With this error equation at hand we now proceed to control the contributions of η_K. We begin with $\boldsymbol{R}_K$. Let $K\in\mathscr{T}$. In view of (39) and (54), a simple application of the triangle inequality reveals that

$$\|\boldsymbol{R}_K\|_{\boldsymbol{L}^2(K)} \leq \|\hat{\boldsymbol{R}}_K\|_{\boldsymbol{L}^2(K)} + \|\mathbf{osc}_K\|_{\boldsymbol{L}^2(K)}. \quad (56)$$

It thus suffices to bound $\hat{\boldsymbol{R}}_K$ To accomplish this task, we set $\boldsymbol{v} = \beta_K \hat{\boldsymbol{R}}_K$ as test function in (55). This yields

$$\|\hat{\boldsymbol{R}}_K\|^2_{\boldsymbol{L}^2(K)} \leq \left|\mathcal{A}(t;\boldsymbol{u},\beta_K\hat{\boldsymbol{R}}_K) - \mathcal{A}(t_{\mathscr{T}};\boldsymbol{u}_{\mathscr{T}},\beta_K\hat{\boldsymbol{R}}_K)\right| + \left|\mathcal{C}(\boldsymbol{u};\boldsymbol{u},\beta_K\hat{\boldsymbol{R}}_K) - \mathcal{C}(\boldsymbol{u}_{\mathscr{T}};\boldsymbol{u}_{\mathscr{T}},\beta_K\hat{\boldsymbol{R}}_K)\right| + \left|\mathcal{B}(\beta_K\hat{\boldsymbol{R}}_K,e_p) + \mathcal{D}(e_t,\beta_K\hat{\boldsymbol{R}}_K) + (\mathbf{osc}_K,\beta_K\hat{\boldsymbol{R}}_K)_{L^2(\Omega)}\right| =: \mathrm{I}+\mathrm{II}+\mathrm{III}. \quad (57)$$

We proceed to estimate the terms on the right-hand side of the previous expression. We begin with the control of I. In fact, rewriting the difference in I as in (29), we arrive at

$$\begin{aligned}\mathrm{I} &= \left|\mathcal{A}(t;\boldsymbol{e_u},\beta_K\hat{\boldsymbol{R}}_K) + \left[(\mathcal{A}(t;\boldsymbol{u},\beta_K\hat{\boldsymbol{R}}_K) - \mathcal{A}(t_{\mathscr{T}};\boldsymbol{u},\beta_K\hat{\boldsymbol{R}}_K)) - (\mathcal{A}(t;\boldsymbol{e_u},\beta_K\hat{\boldsymbol{R}}_K) - \mathcal{A}(t_{\mathscr{T}};\boldsymbol{e_u},\beta_K\hat{\boldsymbol{R}}_K))\right]\right| \\ &\leq C\left[|\boldsymbol{e_u}|_{\boldsymbol{H}^1(K)} + \|e_t\|_{H^1(K)}\left(\|\nabla\boldsymbol{u}\|_{\boldsymbol{L}^3(K)} + \|\nabla\boldsymbol{e_u}\|_{\boldsymbol{L}^3(K)}\right)\right]|\beta_K\hat{\boldsymbol{R}}_K|_{\boldsymbol{H}^1(K)} \\ &\leq C\left(|\boldsymbol{e_u}|_{\boldsymbol{H}^1(K)} + \|e_t\|_{H^1(K)}\right)h_K^{-1}\|\beta_K\hat{\boldsymbol{R}}_K\|_{\boldsymbol{L}^2(K)},\end{aligned}$$

where we have used local version of the estimates (12) and (15), an assumption from (30), and an inverse inequality. Second, applying similar arguments, we estimate the terms related with the nonlinear convective derivatives. In fact, we have that

$$\begin{aligned}\mathrm{II} &= |\mathcal{C}(\boldsymbol{u};\boldsymbol{e_u},\beta_K\hat{\boldsymbol{R}}_K) - \mathcal{C}(\boldsymbol{e_u};\boldsymbol{e_u},\beta_K\hat{\boldsymbol{R}}_K) + \mathcal{C}(\boldsymbol{e_u};\boldsymbol{u},\beta_K\hat{\boldsymbol{R}}_K)| \\ &\leq C\left[\|\boldsymbol{u}\|_{\boldsymbol{H}^1(K)}|\boldsymbol{e_u}|_{\boldsymbol{H}^1(K)} + \|\boldsymbol{e_u}\|_{\boldsymbol{H}^1(K)}\left(|\boldsymbol{e_u}|_{\boldsymbol{H}^1(K)} + |\boldsymbol{u}|_{\boldsymbol{H}^1(K)}\right)\right]\|\beta_K\hat{\boldsymbol{R}}_K\|_{\boldsymbol{H}^1(K)} \\ &\leq C\|\boldsymbol{e_u}\|_{\boldsymbol{H}^1(K)}(1+h_K^{-1})\|\beta_K\hat{\boldsymbol{R}}_K\|_{\boldsymbol{L}^2(K)}.\end{aligned}$$

Finally, we control the term III on the basis of (20):

$$\begin{aligned}\mathrm{III} &\leq C\left(\|e_p\|_{L^2(K)} + \|\boldsymbol{g}\|_{\boldsymbol{L}^2(\Omega)}\|e_t\|_{H^1(K)}+\right)\|\beta_K\hat{\boldsymbol{R}}_K\|_{\boldsymbol{H}^1(K)} + \|\mathbf{osc}_K\|_{\boldsymbol{L}^2(K)}\|\beta_K\hat{\boldsymbol{R}}_K\|_{\boldsymbol{L}^2(K)} \\ &\leq C\left(\|e_p\|_{L^2(K)} + \|e_t\|_{H^1(K)}\right)(1+h_K^{-1})\|\beta_K\hat{\boldsymbol{R}}_K\|_{\boldsymbol{L}^2(K)} + \|\mathbf{osc}_K\|_{\boldsymbol{L}^2(K)}\|\beta_K\hat{\boldsymbol{R}}_K\|_{\boldsymbol{L}^2(K)}.\end{aligned}$$

Gathering the previous results and utilizing (52), we conclude that

$$h_K^2\|\hat{\boldsymbol{R}}_K\|^2_{\boldsymbol{L}^2(K)} \leq C\Big((1+h_K^2)\left(\|\boldsymbol{e_u}\|^2_{\boldsymbol{H}^1(K)} + \|e_p\|^2_{L^2(K)} + \|e_t\|^2_{H^1(K)}\right) + h_K^2\|\mathbf{osc}_K\|^2_{\boldsymbol{L}^2(K)}\Big), \quad (58)$$

In view of (56), $h_K^2\|\boldsymbol{R}_K\|^2_{\boldsymbol{L}^2(K)}$ can also be controlled with the right-hand side of (58).

If $\gamma \in \mathcal{F}_K \cap \mathcal{F}_{K'}$ with $K \neq K'$ and $K, K' \in \mathscr{T}$, we set in (55) $\boldsymbol{v} = \beta_\gamma \boldsymbol{J}_\gamma$, which is supported in Ω_γ. Similar arguments to the ones that we have previously used combined with (53) allow us to conclude that

$$h_K\|\boldsymbol{J}_\gamma\|^2_{\boldsymbol{L}^2(\gamma)} \leq C\left(\sum_{K\in\Omega_\gamma}(1+h_K^2)\left(\|\boldsymbol{e_u}\|^2_{\boldsymbol{H}^1(K)} + \|e_p\|^2_{L^2(K)} + \|e_t\|^2_{H^1(K)}\right) + h_K^2\|\mathbf{osc}_K\|^2_{\boldsymbol{L}^2(K)}\right). \quad (59)$$

Step 2: We now proceed to bound the term $\|\nabla\cdot\boldsymbol{u}_{\mathscr{T}}\|_{L^2(K)}$. In fact, using that $\boldsymbol{u} \in \boldsymbol{X}(\Omega)$, we immediately arrive at the estimate

$$\|\nabla\cdot\boldsymbol{u}_{\mathscr{T}}\|_{L^2(K)} := \|\nabla\cdot\boldsymbol{e_u}\|_{L^2(K)} \leq d|\boldsymbol{e_u}|_{\boldsymbol{H}^1(K)}.$$

Step 3: For $K \in \mathscr{T}$, we define the following residual and oscillation terms:

$$\left\{\begin{array}{rcl}\hat{R}_K &:=& \Pi_{K,1}(h) + \mathrm{div}(\kappa(t_{\mathscr{T}})\nabla t_{\mathscr{T}})_{|K} - \boldsymbol{u}_{\mathscr{T}|K}\cdot\nabla t_{\mathscr{T}|K}, \\ \mathrm{osc}_K &:=& h - \Pi_{K,1}(h).\end{array}\right. \quad (60)$$

With this definiton at hand, we invoke the definitions of R_K and J_γ, given in (43), the definitions of the forms $\mathscr{A}$ and $\mathscr{C}$, given in (9), and an integration by parts formula to conclude the following error equation, which holds for $w \in H_0^1(\Omega)$:

$$\sum_{K\in\mathscr{T}}\int_K \hat{R}_K w - \sum_{\gamma\in\mathcal{F}_I}\int_\gamma J_\gamma w = \mathscr{A}(t;t,w) - \mathscr{A}(t_{\mathscr{T}};t_{\mathscr{T}},w) + \mathscr{C}(\boldsymbol{u};t,w) - \mathscr{C}(\boldsymbol{u}_{\mathscr{T}};t_{\mathscr{T}},w) - \sum_{K\in\mathscr{T}}\int_K \mathrm{osc}_K w. \quad (61)$$

Set $w = \beta_K\hat{R}_K$ as a test function in (61). We apply similar arguments to the ones developed in *Step 1* to conclude that

$$\mathscr{A}(t;t,\beta_K\hat{R}_K)-\mathscr{A}(t_{\mathscr{T}};t_{\mathscr{T}},\beta_K\hat{R}_K)$$
$$\leq C\left(|e_t|_{H^1(K)}+\|e_t\|_{H^1(K)}\left(\|\nabla t\|_{L^3(K)}+\|\nabla e_t\|_{L^3(K)}\right)\right)|\beta_K\hat{R}_K|_{H^1(K)}\leq C\|e_t\|_{H^1(K)}|\beta_K\hat{R}_K|_{H^1(K)},$$

and that

$$\begin{aligned}\mathscr{C}(\boldsymbol{u};t,w)-\mathscr{C}(\boldsymbol{u}_{\mathscr{T}};t_{\mathscr{T}},w)&\leq C\left(|e_t|_{H^1(K)}\left(\|\boldsymbol{u}\|_{\boldsymbol{H}^1(K)}+\|\boldsymbol{e_u}\|_{\boldsymbol{H}^1(K)}\right)+|t|_{H^1(K)}\|\boldsymbol{e_u}\|_{\boldsymbol{H}^1(K)}\right)\|\beta_K\hat{R}_K\|_{H^1(K)}\\&\leq C\left(|e_t|_{H^1(K)}+\|\boldsymbol{e_u}\|_{\boldsymbol{H}^1(K)}\right)\|\beta_K\hat{R}_K\|_{H^1(K)}.\end{aligned}$$

Combining the derived bounds with (52) and (53), we conclude that

$$h_K^2\|R_K\|_{L^2(K)}^2\leq C\left((1+h_K^2)\left(\|e_t\|_{H^1(K)}^2+\|\boldsymbol{e_u}\|_{\boldsymbol{H}^1(K)}^2\right)+h_K^2\|\mathrm{osc}_K\|_{L^2(K)}^2\right),$$
$$h_K\|R_\gamma\|_{L^2(\gamma)}^2\leq C\sum_{K\in\Omega_\gamma}\left((1+h_K^2)\left(\|e_t\|_{H^1(K)}^2+\|\boldsymbol{e_u}\|_{\boldsymbol{H}^1(K)}^2\right)+h_K^2\|\mathrm{osc}_K\|_{L^2(K)}^2\right).$$

Gathering all of our previous finding we conclude the desired estimate. □

We conclude with the following result.

Theorem 7 (local efficiency)**.** *Let $(\boldsymbol{u},p,t)$ be the solution to* (8) *and $(\mathfrak{L}(\boldsymbol{u}_{\mathscr{T}},p_{\mathscr{T}}),p_{\mathscr{T}},t_{\mathscr{T}})$ its nonconforming finite element approximation which enriches the velocity field as described in* (26)*. If $p\in H^1(\Omega)$ and* (30) *holds, then the error indicator Θ_K, given as in* (50)*, satisfies, for every $K\in\mathscr{T}$, that*

$$\Theta_K^2\leq C\sum_{\gamma\in\mathcal{F}_K}\sum_{K'\in\Omega_\gamma}(1+h_K^2)\Bigg(\|\boldsymbol{e_u}\|_{\boldsymbol{H}^1(K')}^2+\|e_p\|_{L^2(K')}^2+\|e_t\|_{H^1(K')}^2$$
$$+h_{K'}^2\left(|e_p|_{H^1(K')}^2+\|\mathbf{osc}_{K'}\|_{\boldsymbol{L}^2(K')}^2+\|\mathrm{osc}_{K'}\|_{L^2(K')}^2\right)\Bigg).$$

Proof. Since $p\in H^1(\Omega)$, we have, for $\gamma\in\mathcal{F}_I$, that $[\![p]\!]=0$. Consequently, $h_K\|[\![p_{\mathscr{T}}]\!]\|_{L^2(\gamma)}^2=h_K\|[\![e_p]\!]\|_{L^2(\gamma)}^2$. Since $h_\gamma\leq Ch_K$, due to the mesh regularity, we apply a scaled trace inequality to arrive at

$$h_K\|[\![p_{\mathscr{T}}]\!]\|_{L^2(\gamma)}^2=h_K\|[\![e_p]\!]\|_{L^2(\gamma)}^2\leq C\sum_{K\in\Omega_\gamma}\left(\|e_p\|_{L^2(K)}^2+h_K^2|e_p|_{H^1(K)}^2\right).$$

The result then follows from using the previous bound combined with the results of Theorem 6. □

6. Numerical examples

In this section we conduct a series of numerical examples that illustrate the performance of the a posteriori error estimators that we have desgined and analyzed in previous sections. All the numerical experiments have been carried out with the help of a code that we implemented using `C++`. All matrices have been assembled exactly. The right hand sides and approximation errors are computed by a quadrature formula which is exact for polynomials of degree 14. The global linear systems were solved using the multifrontal massively parallel sparse direct solver (MUMPS) [10, 11]. The graphical representations of the obtained finite element solutions were performed with the help of `ParaView` [1].

For when the solution technique **SFEM1** is considered, we measure experimental rates of convergence for the error in the energy-type norms:

$$\|(\boldsymbol{\xi},\phi)\|_{\mathcal{F}}^2:=|\boldsymbol{\xi}|_{\boldsymbol{H}^1(\Omega)}^2+\|\phi\|_{L^2(\Omega)}^2,\quad |||(\boldsymbol{\xi},\phi,\theta)|||^2=\|(\boldsymbol{\xi},\phi)\|_{\mathcal{F}}^2+|e_t|_{H^1(\Omega)}^2.$$

When the scheme **SFEM2** is considered, we employ the following broken norms for measuring experimental rates of convergence:

$$\|(\boldsymbol{\xi},\phi)\|_{\mathcal{F}(\mathscr{T})}^2:=|\boldsymbol{\xi}|_{\boldsymbol{H}^1(\mathscr{T})}^2+\|\phi\|_{L^2(\Omega)}^2,\quad |||(\boldsymbol{\xi},\phi,\theta)|||_{\mathscr{T}}^2=\|(\boldsymbol{\xi},\phi)\|_{\mathcal{F}(\mathscr{T})}^2+|e_t|_{H^1(\Omega)}^2,$$

where $|\cdot|_{\boldsymbol{H}^1(\mathscr{T})}$ is defined in (49). We denote by NDOF the total number of degrees of freedom, which is given by

$$\mathrm{NDOF}=\#(\mathbf{V}(\mathscr{T}))+\#(Q(\mathscr{T}))+\#(V(\mathscr{T})).$$

We solve the discrete system (25) on the basis of the fix–point strategy presented in [5, Section 6]. We thus calculate the local error indicators η_K, for when we consider the **SFEM1** scheme, or the local error

indicators Θ_K for when the **SFEM2** scheme is considered, in order to drive an adaptive mesh refinement procedure, and the global error estimator η (Θ), in order to assess the accuracy of the approximation. The following refinement criterion was used: Mark an element K for refinement if

$$\eta_K^2 \geq 0.5 \max_{K' \in \mathscr{T}} \eta_{K'}^2 \quad (\Theta_K^2 \geq 0.5 \max_{K' \in \mathscr{T}} \Theta_{K'}^2). \tag{62}$$

The adaptive loop generates a sequence of adaptive meshes on which experimental rates of convergence were computed.

To measure the aforementioned experimental rates of convergence for the error, we construct exact solutions for problem (8) that are based on the following functions:

$$\boldsymbol{u}_1(x,y,z) = \mathbf{curl}\left[(xy(1-x)(1-y)z(1-z))^2 \boldsymbol{e}_1\right],$$
$$\boldsymbol{u}_2(x,y,z) = \mathbf{curl}\left[xy(1-x)(1-y)\left(z - \frac{e^{-(1-z)/\varepsilon} - e^{-1/\varepsilon}}{1-e^{-1/\varepsilon}}\right)^2 \boldsymbol{e}_3\right],$$
$$p_1(x,y,z) = xyz - 1/8, \quad p_2(x,y,z) = xyz(1-x)(1-y)(1-z) - 1/216,$$
$$t_1(x,y,z) = xyz(1-x)(1-y)(1-z), \quad t_2(x,y,z) = xyz(1-x)(1-y)(1-z)\arctan\left(\frac{x-0.5}{\kappa}\right),$$

where $\boldsymbol{e}_1 = [1\ 0\ 0]$, and $\boldsymbol{e}_3 = [0\ 0\ 1]$.

As is customary in a posteriori error analysis, in order to measure the efficiency of the involved adaptive algorithm, with respect to the error norm, we consider the following effectivity indices:

$$\mathtt{ef}_1 = \frac{\eta}{|||(\boldsymbol{e}_{\boldsymbol{u}}, e_p, e_t)|||}, \quad \mathtt{ef}_2 = \frac{\Theta}{|||(\boldsymbol{e}_{\boldsymbol{u}}, e_p, e_t)|||_{\mathscr{T}}}.$$

Finally, we mention that in all of our numerical examples we have chosen, as stabilization parameters, $\tau = \tilde{\tau} = 1$.

6.1. **The Stokes equation coupled with a convection–diffusion equation.** We first consider a simplified version of (5) that correspond to a system of PDEs that couples the homogeneous problem for the incompressible Stokes system with a convection-diffusion equation. To be precise, we consider the following system of PDEs

$$\left\{\begin{array}{rcll} -\varepsilon\Delta\boldsymbol{u} + \nabla p - \boldsymbol{g}t &=& \boldsymbol{f} & \text{in } \Omega, \\ \mathbf{div}\,\boldsymbol{u} &=& 0 & \text{in } \Omega, \\ -\kappa\Delta t + \boldsymbol{u}\cdot\nabla t &=& h & \text{in } \Omega, \\ \boldsymbol{u} &=& 0 & \text{on } \Gamma, \\ t &=& 0 & \text{on } \Gamma, \end{array}\right. \tag{63}$$

with ε and κ being positive constants. On the basis of similar arguments to the ones developed in Section 5.1, and in particular in Theorem 2, the following estimate can be derived:

$$\varepsilon|\boldsymbol{e}_{\boldsymbol{u}}|^2_{\boldsymbol{H}^1(\Omega)} + \frac{1}{\varepsilon}\|e_p\|^2_{L^2(\Omega)} + \kappa|e_t|^2_{H^1(\Omega)} \leq C\left(\varepsilon|\boldsymbol{\Phi}|^2_{\boldsymbol{H}^1(\Omega)} + \frac{1}{\varepsilon}\|\psi\|^2_{L^2(\Omega)} + \kappa|\varphi|^2_{H^1(\Omega)}\right). \tag{64}$$

The a posteriori error analysis that we have performed can be adapted to this simplified case. In fact, when the **SFEM1** scheme is considered, the following a posteriori error estimator can be designed

$$\omega^2 = \sum_{K\in\mathscr{T}} \omega_K^2, \qquad \omega_K^2 = \omega_{F,K}^2 + \omega_{T,K}^2, \qquad \omega_F^2 = \sum_{K\in\mathscr{T}} \omega_{F,K}^2, \qquad \omega_T^2 = \sum_{K\in\mathscr{T}} \omega_{T,K}^2.$$

The error indicators $\omega_{F,K}$ and $\omega_{F,T}$ are given by

$$\omega_{F,K}^2 := \frac{h_K^2}{\varepsilon}\|\boldsymbol{R}_K\|^2_{\boldsymbol{L}^2(K)} + \frac{1}{\varepsilon}\left(1+\tau^2 h_K^2\right)\|\nabla\cdot\boldsymbol{u}_{\mathscr{T}}\|^2_{L^2(K)} + \sum_{\gamma\in\mathcal{F}_K\cap\mathcal{F}_I} \frac{h_K}{\varepsilon}\|\boldsymbol{J}_{\gamma,K}\|^2_{\boldsymbol{L}^2(\gamma)},$$

$$\omega_{T,K}^2 := \frac{h_K^2}{\kappa}\|R_K\|^2_{L^2(K)} + \sum_{\gamma\in\mathcal{F}_K\cap\mathcal{F}_I} \frac{h_K}{\kappa}\left(1+\tilde{\tau}h_K^3\right)\|J_{\gamma,K}\|^2_{L^2(\gamma)},$$

with obvious modifications for the terms $\boldsymbol{R}_K$ and $\boldsymbol{J}_{\gamma,K}$. We recall that τ and $\tilde{\tau}$ denote stabilization parameters. For the **SFEM2** solution technique, we design the following error estimator and error indicators to drive adaptive procedures:

$$\Xi^2 := \sum_{K\in\mathscr{T}} \Xi_K^2, \qquad \Xi_K^2 = \Xi_{F,K}^2 + \Xi_{T,K}^2, \qquad \Xi_F^2 := \sum_{K\in\mathscr{T}} \Xi_{F,K}^2, \qquad \Xi_T^2 := \sum_{K\in\mathscr{T}} \Xi_{T,K}^2,$$

with

$$\Xi_{F,K}^2 := \frac{h_K^2}{\varepsilon}\|\boldsymbol{R}_K\|_{\boldsymbol{L}^2(K)}^2 + \frac{1}{\varepsilon}\left(1+\tau^2 h_K^2\right)\|\nabla\cdot\boldsymbol{u}_{\mathscr{T}}\|_{L^2(K)}^2 + \sum_{\gamma\in\mathcal{F}_K\cap\mathcal{F}_I} h_K\left(\frac{1}{\varepsilon}\|\boldsymbol{J}_{\gamma,K}\|_{\boldsymbol{L}^2(\gamma)}^2 + \varepsilon\|[\![p_{\mathscr{T}}]\!]\|_{L^2(\gamma)}^2\right),$$

$$\Xi_{T,K}^2 := \frac{h_K^2}{\kappa}\|R_K\|_{L^2(K)}^2 + \sum_{\gamma\in\mathcal{F}_K\cap\mathcal{F}_I}\frac{h_K}{\kappa}\left(1+\tilde{\tau}h_K^3\right)\|J_{\gamma,K}\|_{L^2(\gamma)}^2.$$

The marking criteria (62) is used to drive the underlying adaptive procedure.

Finally, we mention that the norms used to measure experimental rates of convergence for the error need to be suitable modified. In fact,

$$\|(\boldsymbol{\xi},\phi)\|_{\mathcal{F}}^2 := \varepsilon|\boldsymbol{\xi}|_{\boldsymbol{H}^1(\Omega)}^2 + \frac{1}{\varepsilon}\|\phi\|_{L^2(\Omega)}^2, \quad |||(\boldsymbol{\xi},\phi,\theta)|||^2 = \|(\boldsymbol{\xi},\phi)\|_{\mathcal{F}}^2 + \kappa|\theta|_{H^1(\Omega)}^2,$$

for when the **SFEM1** method is chosen, and

$$\|(\boldsymbol{\xi},\phi)\|_{\mathcal{F}(\mathscr{T})}^2 := \varepsilon|\boldsymbol{\xi}|_{\boldsymbol{H}^1(\mathscr{T})}^2 + \frac{1}{\varepsilon}\|\phi\|_{L^2(\Omega)}^2, \quad |||(\boldsymbol{\xi},\phi,\theta)|||_{\mathscr{T}}^2 = \|(\boldsymbol{\xi},\phi)\|_{\mathcal{F}(\mathscr{T})}^2 + \kappa|\theta|_{H^1(\Omega)}^2,$$

for when the **SFEM2** solution is considered.

To measure the efficiency of the involved adaptive algorithm we introduce the following effectivity indices

$$\widetilde{\mathtt{ef}}_1 = \frac{\omega}{|||(\boldsymbol{e}_{\boldsymbol{u}},e_p,e_t)|||}, \quad \widetilde{\mathtt{ef}}_2 = \frac{\Xi}{|||(\boldsymbol{e}_{\boldsymbol{u}},e_p,e_t)|||_{\mathscr{T}}}.$$

Example 1: We let $\Omega = (0,1)^3$, $\varepsilon = 10^{-3}$, $\kappa = 10^{-3}$, and $\boldsymbol{g} = (0,0,1)^T$. The forcing terms $\boldsymbol{f}$ and h are such that the exact solution to (8) reads

$$\boldsymbol{u}(x,y,z) = \boldsymbol{u}_2(x,y,z), \qquad p(x,y) = p_2(x,y,z) \qquad t(x,y) = t_2(x,y,z).$$

Example 2: We let $\Omega = (0,1)^3$, $\varepsilon = 1$, $\kappa = 1$, $\boldsymbol{f} \equiv \boldsymbol{0}$, and $h \equiv 0$. We explore the performance of the devised a posteriori error estimators in a setting that goes beyond the presented theory: the so-called differentially heated cavity flow problem. To be precise, we consider problem (63), but with the boundary conditions as stated in Figure 3. We also set

$$\boldsymbol{g} = (0,0,Ra)^T,$$

where Ra corresponds to the Rayleigh's number. The latter is associated with the heat transfer inside the fluid; a low value for Ra implies that the conduction transfer is dominant, while a high value of Ra ($Ra > 1000$) implies that the convection transfer is dominant. In this specific example we set $Ra = 10^5$.

In Figure 2 we present the results obtained for Example 1: experimental rates of convergence for error and error estimators, their individual contributions, and the effectivity index $\widetilde{\mathtt{ef}}_2$. We also present graphic representations of the involved discrete functions and slices of the final mesh which contains 1025888 elements and 182633 vertices. Similar results are presented, for Example 2, in Figure 4.

6.2. **The generalized Boussinesq problem.**

Example 3: We let $\Omega = (0,1)^3$, $\varepsilon(t) = e^{-t}$, $\kappa(t) = e^t$, and $\boldsymbol{g} = (0,0,1)^T$. The terms $\boldsymbol{f}$ and h are such that

$$\boldsymbol{u}(x,y,z) = \boldsymbol{u}_1(x,y,z), \qquad p(x,y,z) = p_1(x,y,z), \qquad t(x,y,z) = t_1(x,y,z).$$

In order to present numerical results, we define the following a posteriori error estimators

$$\eta_F^2 := \sum_{K\in\mathscr{T}}\eta_{F,K}^2, \quad \eta_{F,K}^2 := h_K^2\|\boldsymbol{R}_K\|_{\boldsymbol{L}^2(K)}^2 + (1+\tau^2h_K^2)\|\nabla\cdot\boldsymbol{u}_{\mathscr{T}}\|_{L^2(K)}^2 + \sum_{\gamma\in\mathcal{F}_K\cap\mathcal{F}_I} h_K\|\boldsymbol{J}_\gamma\|_{\boldsymbol{L}^2(\gamma)}^2,$$

$$\eta_T^2 := \sum_{K\in\mathscr{T}}\eta_{T,K}^2, \quad \eta_{T,K}^2 := h_K^2\|R_K\|_{L^2(K)}^2 + \sum_{\gamma\in\mathcal{F}_K\cap\mathcal{F}_I} h_K\left(1+\tilde{\tau}h_K^3\right)\|J_\gamma\|_{L^2(\gamma)}^2,$$

and

$$\Theta_F^2 := \sum_{K\in\mathscr{T}}\Theta_{K,F}^2, \quad \Theta_{F,K}^2 := \eta_{F,K}^2 + \sum_{\gamma\in\mathcal{F}_K\cap\mathcal{F}_I} h_K\|[\![p_{\mathscr{T}}]\!]\|_{L^2(\gamma)}^2,$$

$$\Theta_T^2 := \sum_{K\in\mathscr{T}}\Theta_{T,F}^2, \quad \Theta_{T,K}^2 := \eta_{T,K}^2.$$

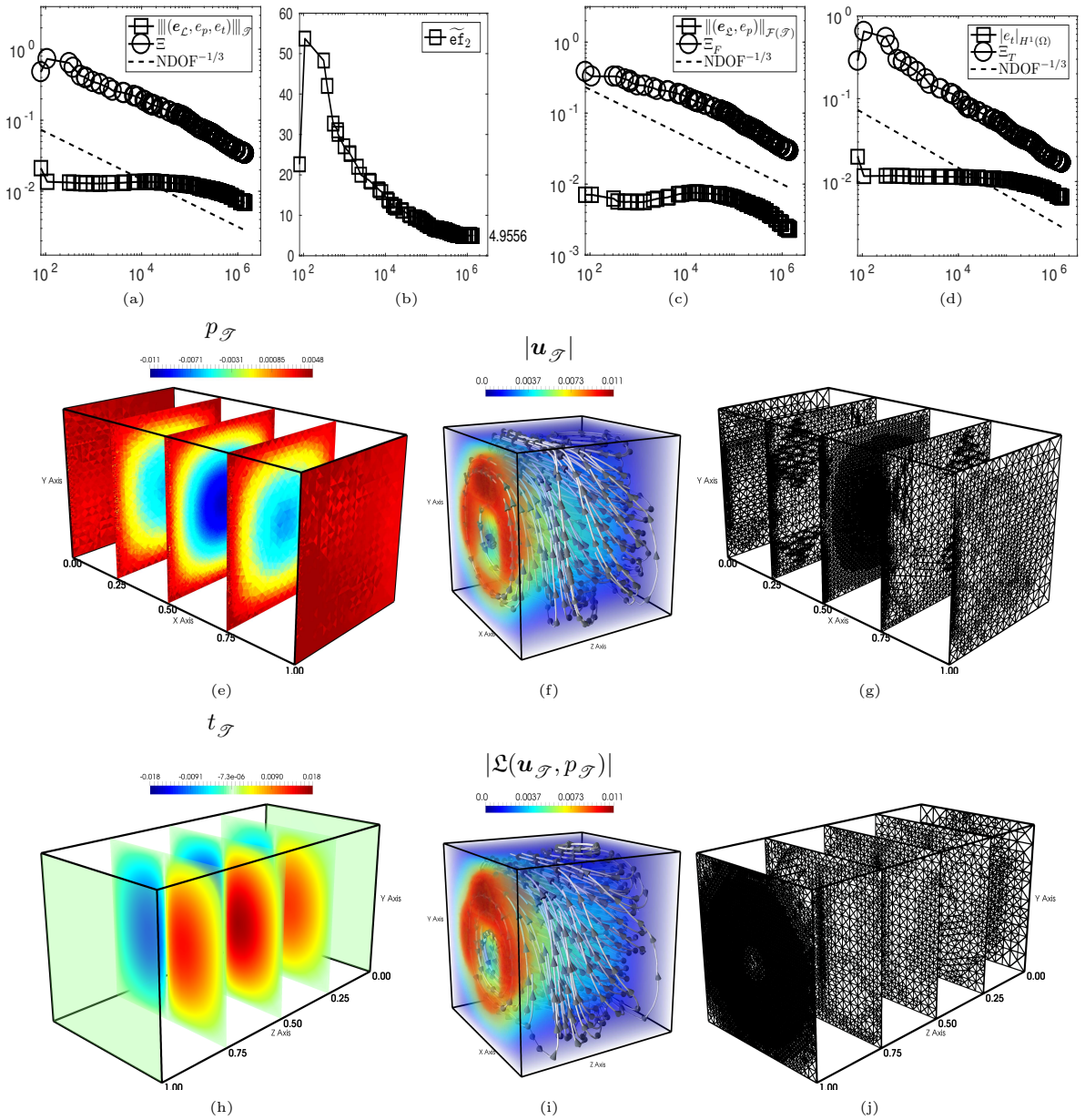

FIGURE 2. Example 1 (**SFEM2** scheme) (a), (b), (c) and (d): Experimental rates of convergence for errors, error estimators, individual contributions, and the effectivity index $\widetilde{\texttt{ef}}_2$. (e): Discrete pressure for fixed and different values of x. (h): Discrete temperature for fixed and different values of z. (f) and (i): Streamlines of the velocity field $\boldsymbol{u}_{\mathscr{T}}$ and $\mathfrak{L}(\boldsymbol{u}_{\mathscr{T}}, p_{\mathscr{T}})$, respectively, combined with its magnitude value. (g) and (j): Slices of the final mesh, that contains 1025888 elements and 182633 vertices, at different fixed values of x and z, respectively.

Notice that the error estimators η and Θ defined by (48) and (50), respectively are such that, $\eta^2 = \eta_F^2 + \eta_T^2$ and $\Theta^2 = \Theta_F^2 + \Theta_T^2$.

Example 4: In this example, we explore the performance of the devised a posteriori error estimators in a setting that goes beyond the presented theory: we consider problem (5) together with the same parameters and boundary conditions as in Example 2.

In Figure 5 we present the results obtained for Example 3: experimental rates of convergence for the error and error estimators, effectivity indices $\texttt{ef}_1$ and $\texttt{ef}_2$, and graphic representations of the involved finite element solutions. Similar results are presented for Example 4 in Figure 6.

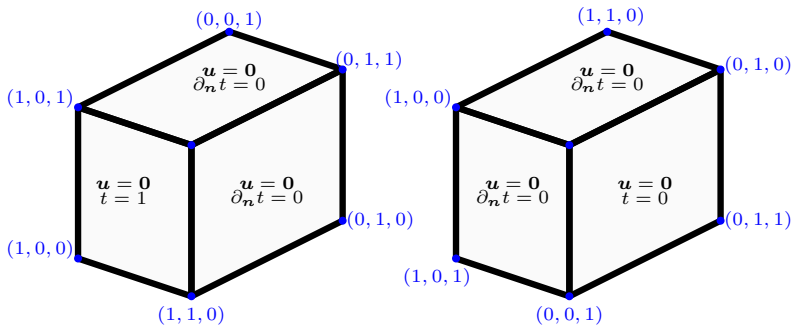

FIGURE 3. Boundary conditions for Example 2 and Example 4, where we have considered $\boldsymbol{g} = (0, 0, Ra)^T$ with $Ra = 10^5$.

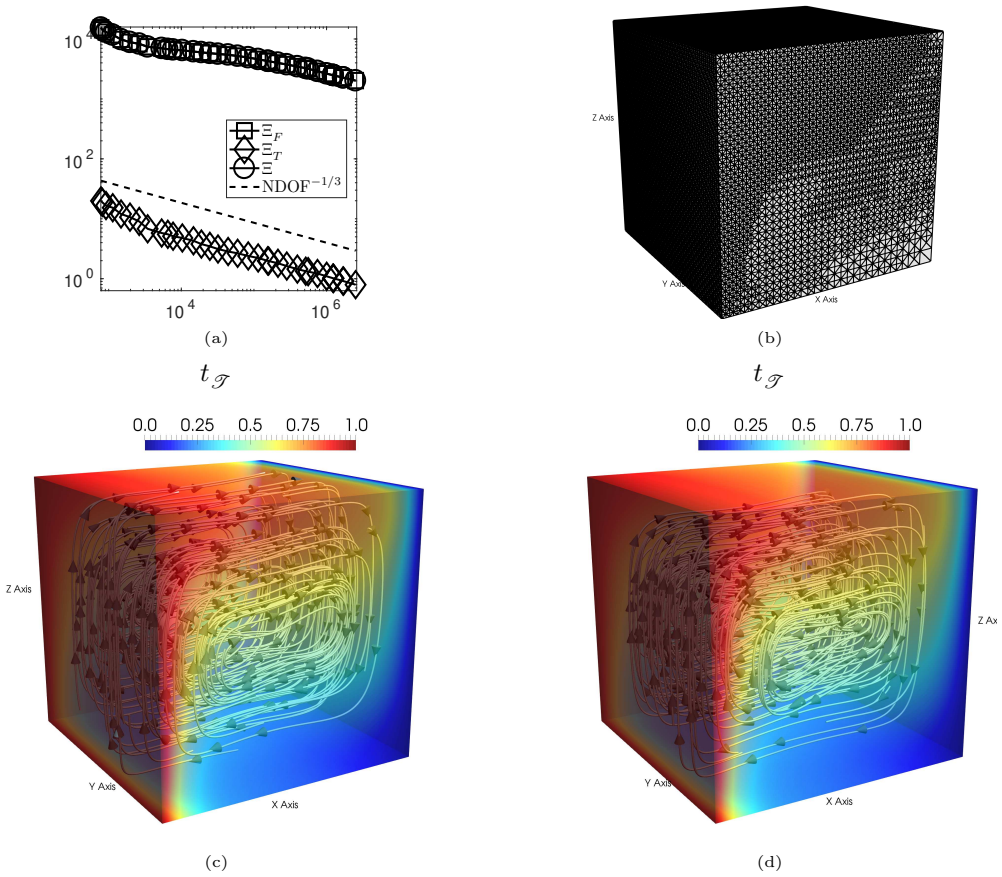

FIGURE 4. Example 2 (**SFEM2** scheme). (a): Experimental rates of convergence for the error estimator Ξ and its individual contributions Ξ_F and Ξ_T. (b): The final mesh: 1454531 elements and 263798 vertices. (c) and (d): Streamlines of the velocity field $\boldsymbol{u}_{\mathscr{T}}$ and $\mathfrak{L}(\boldsymbol{u}_{\mathscr{T}}, p_{\mathscr{T}})$, respectively, combined with a representation of the discrete temperature.

6.3. **Conlusions.** From the presented numerical examples several general conclusions can be drawn:

- We observe optimal experimental rates of convergence for all the total errors, error estimators, and individual contributions.
- The devised error estimators accurately identify boundary and interior layers and direct most of the refinement to these regions.
- In all the numerical experiments that involve an exact solution, the effectivity indices remain bounded. More precisely, when the solution technique start to properly resolve the involved

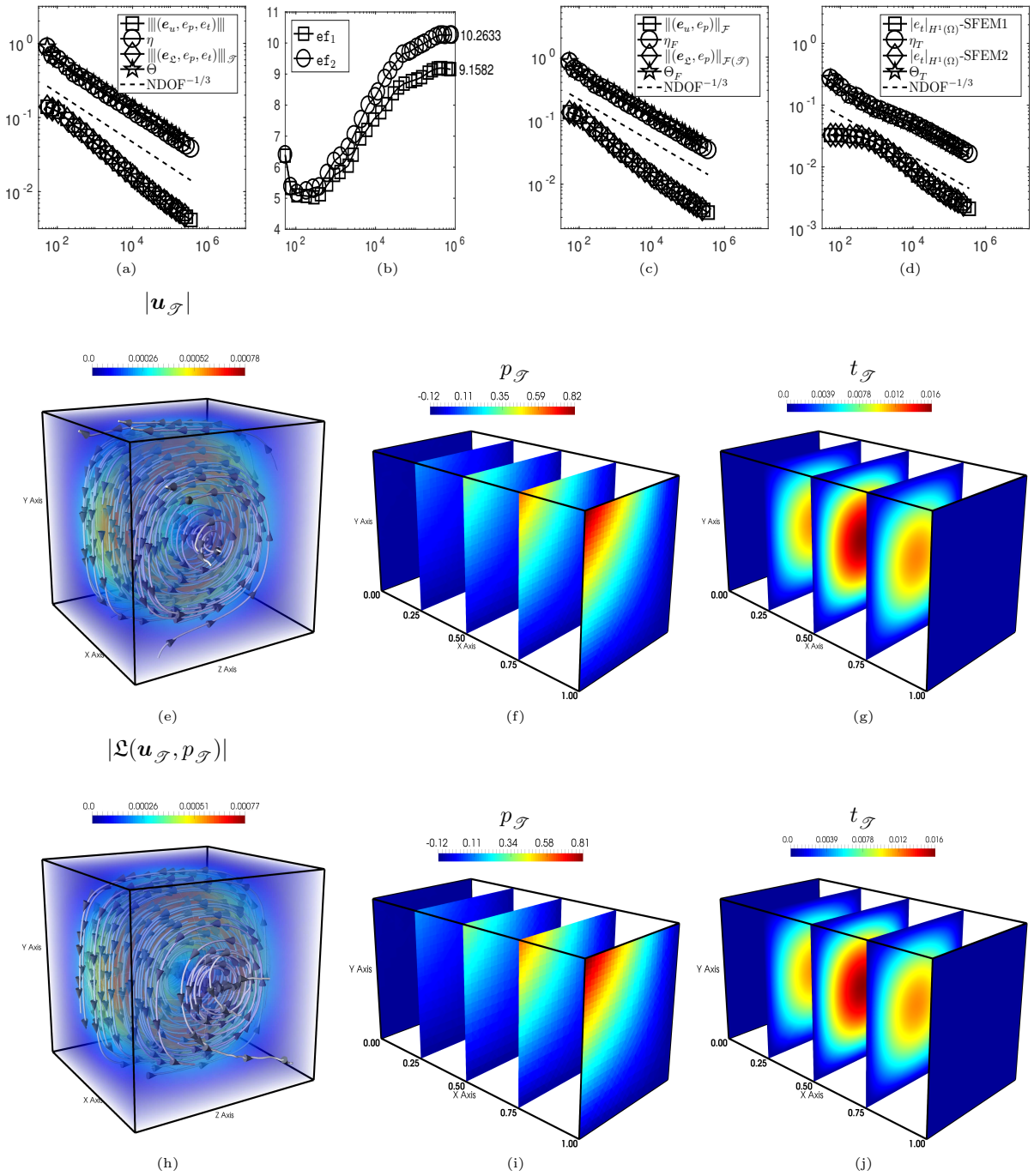

FIGURE 5. Example 3. (a), (b), (c) and (d): Experimental rates of convergence for errors and error estimators, individual contributions, and effectivity indices. (e): Streamlines of the velocity $\boldsymbol{u}_{\mathscr{T}}$ combined with its magnitude value when the **SFEM1** is used; the involved mesh contains 200345 elements and 37857 vertices. (f) and (g): Discrete approximations of the pressure and temperature, respectively, for fixed values of x when the **SFEM1** is used. (h): Streamlines of the velocity $\mathfrak{L}(\boldsymbol{u}_{\mathscr{T}}, p_{\mathscr{T}})$ combined with its magnitude value when the **SFEM2** is used; the involved mesh contains 138243 elements and 26353 vertices. (i) and (j): Discrete approximations of the pressure and temperature, respectively, for fixed values of x when the **SFEM2** is used.

layers, we observe, from Figures 2 and 5, that $\widetilde{\mathtt{ef}}_2 \approx 4.9556$ and $\mathtt{ef}_1 \approx 9.1582$ and $\mathtt{ef}_2 \approx 10.2633$, respectively. These numerical results provide evidence of a competitive performance of the adaptive procedures that are driven by the devised error estimators.

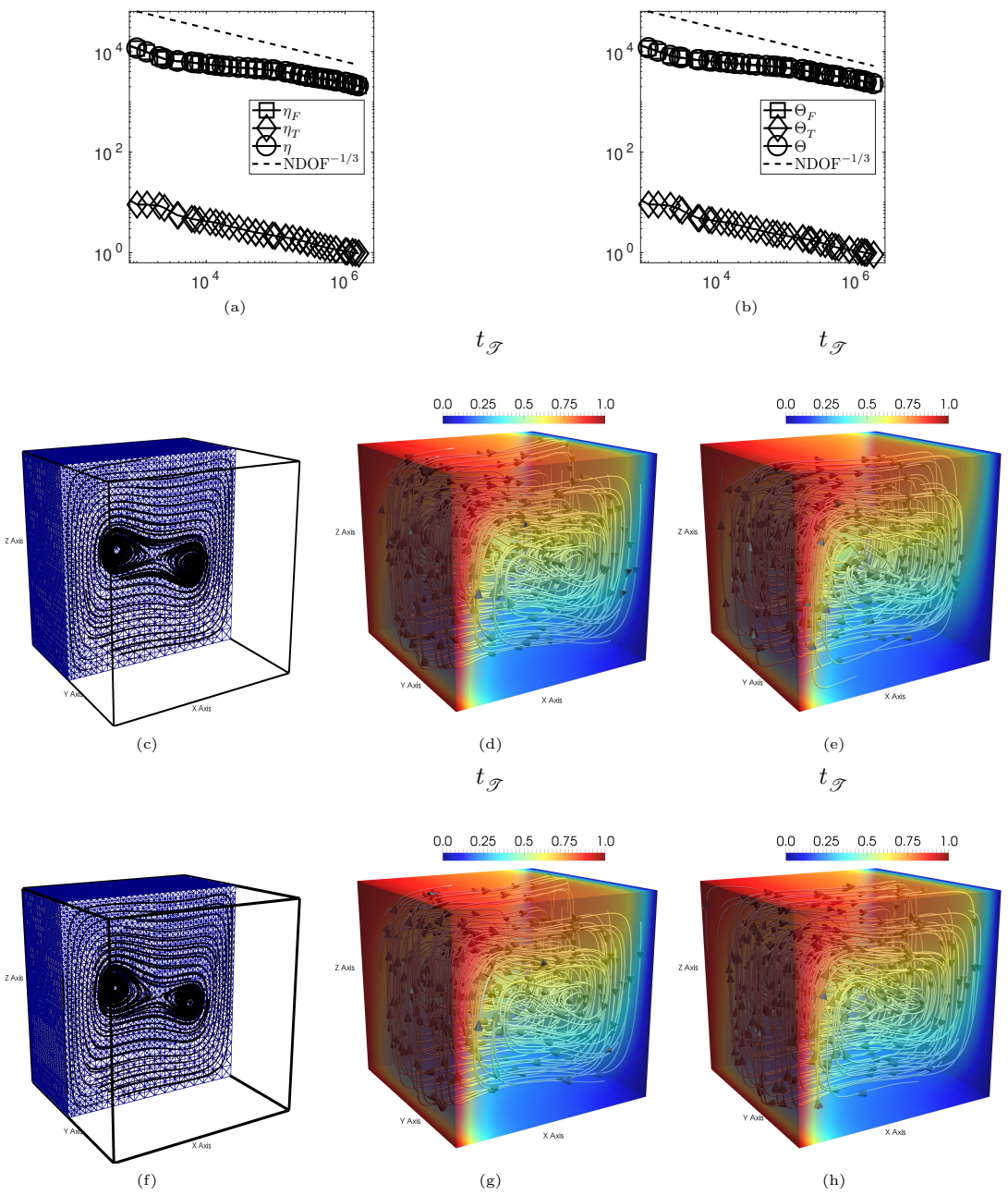

FIGURE 6. Example 4: (a) and (b): Experimental rates of convergence for error estimators and individual contributions. (c): A slice of the streamlines at $y = 0.5$ over the obtained final mesh when the **SFEM1** is used. The mesh contains 895987 elements and 171243 vertices. (f) An analogous representation when the **SFEM2** scheme is employed. The final mesh contains 1009395 elements and 194304 vertices. (d) and (e): Streamlines of the velocity field $\boldsymbol{u}_{\mathscr{T}}$ and $\mathfrak{L}(\boldsymbol{u}_{\mathscr{T}}, p_{\mathscr{T}})$, respectively, combined with a representation of the discrete temperature for the **SFEM1** scheme. (g) and (h) Analogous representations for the **SFEM2** scheme.

- From Figure 5 it can be observed that $\mathtt{ef}_2 > \mathtt{ef}_1$. Notice, in addition, that $|||(\boldsymbol{e}_{\mathfrak{L}}, e_p, e_t)|||_{\mathscr{T}} < |||(\boldsymbol{u}, e_p, e_t)|||$. The following insight could explain why the **SFEM1** scheme is slightly less efficient than the **SFEM2** scheme: notice that the error estimator Θ_K, defined in (50), when compared with η_K, defined in (48), present an extra pressure jump term. Notice, in addition, that both estimators bound the total error.
- In Examples 2 and 4, we consider particular scenarios that go beyond the presented theory. In spite of this fact, optimal experimental rates of convergence are observed.

References

[1] James Ahrens, Berk Geveci, and Charles Law. Paraview: An end-user tool for large data visualization. *The visualization handbook*, 717, 2005.

[2] Mark Ainsworth and J. Tinsley Oden. A posteriori error estimators for the Stokes and Oseen equations. *SIAM J. Numer. Anal.*, 34(1):228–245, 1997.

[3] Mark Ainsworth and J. Tinsley Oden. *A posteriori error estimation in finite element analysis*. Pure and Applied Mathematics (New York). Wiley-Interscience [John Wiley & Sons], New York, 2000.

[4] Karam Allali. A priori and a posteriori error estimates for Boussinesq equations. *Int. J. Numer. Anal. Model.*, 2(2):179–196, 2005.

[5] Alejandro Allendes, Gabriel R. Barrenechea, and César Naranjo. A divergence-free low-order stabilized finite element method for a generalized steady state Boussinesq problem. *Comput. Methods Appl. Mech. Engrg.*, 340:90–120, 2018.

[6] Javier A. Almonacid and Gabriel N. Gatica. A fully–mixed finite element method for the n-dimensional Boussinesq problem with temperature–dependent parameters.

[7] Javier A. Almonacid, Gabriel N. Gatica, and Ricardo Oyarzúa. A mixed–primal finite element method for the Boussinesq problem with temperature-dependent viscosity. *Calcolo*, 55(3):Art. 36, 42, 2018.

[8] Javier A. Almonacid, Gabriel N. Gatica, and Ricardo Oyarzúa. A Posteriori Error Analysis of a Mixed-Primal Finite Element Method for the Boussinesq Problem with Temperature-Dependent Viscosity. *J. Sci. Comput.*, 78(2):887–917, 2019.

[9] Javier A. Almonacid, Gabriel N. Gatica, Ricardo Oyarzúa, and Ricardo Ruiz-Baier. A new mixed finite element method for the n-dimensional Boussinesq problem with temperature-dependent viscosity. 2018.

[10] Patrick R. Amestoy, Iain S. Duff, and Jean-Yves L'Excellent. Multifrontal parallel distributed symmetric and unsymmetric solvers. *Comput. Methods in Appl. Mech. Eng.*, 184(24):501 – 520, 2000.

[11] Patrick R. Amestoy, Iain S. Duff, Jean-Yves L'Excellent, and Jacko Koster. A fully asynchronous multifrontal solver using distributed dynamic scheduling. *SIAM J. Matrix Anal. Appl.*, 23(1):15–41, 2001.

[12] Gabriel R. Barrenechea and Frédéric Valentin. Consistent local projection stabilized finite element methods. *SIAM J. Numer. Anal.*, 48(5):1801–1825, 2010.

[13] Christine Bernardi, Brigitte Métivet, and Bernadette Pernaud-Thomas. Couplage des équations de Navier-Stokes et de la chaleur: le modèle et son approximation par éléments finis. *RAIRO Modél. Math. Anal. Numér.*, 29(7):871–921, 1995.

[14] J. Boland and W. Layton. An analysis of the finite element method for natural convection problems. *Numer. Methods Partial Differential Equations*, 6(2):115–126, 1990.

[15] Erik Burman and Peter Hansbo. Edge stabilization for Galerkin approximations of convection-diffusion-reaction problems. *Comput. Methods Appl. Mech. Engrg.*, 193(15-16):1437–1453, 2004.

[16] Aytekin Çı bık and Songül Kaya. A projection-based stabilized finite element method for steady-state natural convection problem. *J. Math. Anal. Appl.*, 381(2):469–484, 2011.

[17] Philippe G. Ciarlet. *The finite element method for elliptic problems*, volume 40 of *Classics in Applied Mathematics*. Society for Industrial and Applied Mathematics (SIAM), Philadelphia, PA, 2002. Reprint of the 1978 original [North-Holland, Amsterdam; MR0520174 (58 #25001)].

[18] Eligio Colmenares, Gabriel N. Gatica, and Ricardo Oyarzúa. Analysis of an augmented mixed-primal formulation for the stationary Boussinesq problem. *Numer. Methods Partial Differential Equations*, 32(2):445–478, 2016.

[19] Eligio Colmenares, Gabriel N. Gatica, and Ricardo Oyarzúa. An augmented fully-mixed finite element method for the stationary Boussinesq problem. *Calcolo*, 54(1):167–205, 2017.

[20] Eligio Colmenares, Gabriel N. Gatica, and Ricardo Oyarzúa. A posteriori error analysis of an augmented mixed-primal formulation for the stationary Boussinesq model. *Calcolo*, 54(3):1055–1095, 2017.

[21] Eligio Colmenares, Gabriel N. Gatica, and Ricardo Oyarzúa. A posteriori error analysis of an augmented fully-mixed formulation for the stationary Boussinesq model. *Comput. Math. Appl.*, 77(3):693–714, 2019.

[22] Eligio Colmenares and Michael Neilan. Dual-mixed finite element methods for the stationary Boussinesq problem. *Comput. Math. Appl.*, 72(7):1828–1850, 2016.

[23] Alexandre Ern and Jean-Luc Guermond. *Theory and practice of finite elements*, volume 159 of *Applied Mathematical Sciences*. Springer-Verlag, New York, 2004.

[24] M. Farhloul, S. Nicaise, and L. Paquet. A mixed formulation of Boussinesq equations: analysis of nonsingular solutions. *Math. Comp.*, 69(231):965–986, 2000.

[25] Leopoldo P. Franca and Thomas J. R. Hughes. Two classes of mixed finite element methods. *Comput. Methods Appl. Mech. Engrg.*, 69(1):89–129, 1988.

[26] Vivette Girault and Pierre-Arnaud Raviart. *Finite element methods for Navier-Stokes equations*, volume 5 of *Springer Series in Computational Mathematics*. Springer-Verlag, Berlin, 1986. Theory and algorithms.

[27] Pierre Grisvard. *Elliptic problems in nonsmooth domains*, volume 69 of *Classics in Applied Mathematics*. Society for Industrial and Applied Mathematics (SIAM), Philadelphia, PA, 2011. Reprint of the 1985 original [MR0775683].

[28] Pengzhan Huang, Wenqiang Li, and Zhiyong Si. Several iterative schemes for the stationary natural convection equations at different Rayleigh numbers. *Numer. Methods Partial Differential Equations*, 31(3):761–776, 2015.

[29] David Jerison and Carlos E. Kenig. The inhomogeneous Dirichlet problem in Lipschitz domains. *J. Funct. Anal.*, 130(1):161–219, 1995.

[30] Sebastián A. Lorca and José Luiz Boldrini. Stationary solutions for generalized Boussinesq models. *J. Differential Equations*, 124(2):389–406, 1996.

[31] Vladimir Maz'ya and Jürgen Rossmann. *Elliptic equations in polyhedral domains*, volume 162 of *Mathematical Surveys and Monographs*. American Mathematical Society, Providence, RI, 2010.

[32] Marius Mitrea and Matthew Wright. Boundary value problems for the Stokes system in arbitrary Lipschitz domains. *Astérisque*, (344):viii+241, 2012.

[33] Ricardo Oyarzúa, Tong Qin, and Dominik Schötzau. An exactly divergence-free finite element method for a generalized Boussinesq problem. *IMA J. Numer. Anal.*, 34(3):1104–1135, 2014.
[34] Ricardo Oyarzúa and Paulo Zúñiga. Analysis of a conforming finite element method for the Boussinesq problem with temperature-dependent parameters. *J. Comput. Appl. Math.*, 323:71–94, 2017.
[35] Carlos E. Pérez, Jean-Marie Thomas, Serge Blancher, and René Creff. The steady Navier-Stokes/energy system with temperature-dependent viscosity. I. Analysis of the continuous problem. *Internat. J. Numer. Methods Fluids*, 56(1):63–89, 2008.
[36] Carlos E. Pérez, Jean-Marie Thomas, Serge Blancher, and René Creff. The steady Navier-Stokes/energy system with temperature-dependent viscosity. II. The discrete problem and numerical experiments. *Internat. J. Numer. Methods Fluids*, 56(1):91–114, 2008.
[37] Masahisa Tabata and Daisuke Tagami. Error estimates of finite element methods for nonstationary thermal convection problems with temperature-dependent coefficients. *Numer. Math.*, 100(2):351–372, 2005.
[38] Roger Temam. *Navier-Stokes equations. Theory and numerical analysis*. North-Holland Publishing Co., Amsterdam-New York-Oxford, 1977. Studies in Mathematics and its Applications, Vol. 2.
[39] D. J. Tritton. *Physical fluid dynamics*. Oxford Science Publications. The Clarendon Press, Oxford University Press, New York, second edition, 1988.
[40] Rüdiger Verfürth. Robust a posteriori error estimates for stationary convection-diffusion equations. *SIAM J. Numer. Anal.*, 43(4):1766–1782, 2005.
[41] Rüdiger Verfürth. *A posteriori error estimation techniques for finite element methods*. Numerical Mathematics and Scientific Computation. Oxford University Press, Oxford, 2013.
[42] Radyadour Kh. Zeytounian. Joseph boussinesq and his approximation: a contemporary view. *Comptes Rendus Mecanique*, 331(8):575–586, 2003.
[43] Yunzhang Zhang, Yanren Hou, and Hongliang Zuo. A posteriori error estimation and adaptive computation of conduction convection problems. *Appl. Math. Model.*, 35(5):2336–2347, 2011.

AM2V and Departamento de Matemática, Universidad Técnica Federico Santa María, Av. España 1680, Casilla 110-V, Valparaíso, Chile
E-mail address: alejandro.allendes@usm.cl

Departamento de Matemática, Universidad Técnica Federico Santa María, Av. España 1680, Casilla 110-V, Valparaíso, Chile
E-mail address: cesar.naranjo@alumnos.usm.cl

AM2V and Departamento de Matemática, Universidad Técnica Federico Santa María, Av. España 1680, Casilla 110-V, Santiago, Chile
E-mail address: enrique.otarola@usm.cl